# Whole-Cell and Single Channel $K^+$ and $Cl^-$ Currents in Epithelial Cells of Frog Skin

J. FERNANDO GARCÍA-DÍAZ

From the Department of Physiology, Boston University School of Medicine, Boston, Massachusetts 02118

ABSTRACT Whole-cell and single channel currents were studied in cells from frog (*R. pipiens* and *R. catesbiana*) skin epithelium, isolated by collagenase and trypsin treatment, and kept in primary cultures up to three days. Whole-cell currents did not exhibit any significant time-dependent kinetics under any ionic conditions used. With an external K gluconate Ringer solution the currents showed slight inward rectification with a reversal potential near zero and an average conductance of 5 nS at reversal. Ionic substitution of the external medium showed that most of the cell conductance was due to K and that very little, if any, Na conductance was present. This confirmed that most cells originate from inner epithelial layers and contain membranes with basolateral properties. At voltages more positive than 20 mV outward currents were larger with K in the medium than with Na or *N*-methyl-D-glucamine. Such behavior is indicative of a multi-ion transport mechanism. Whole-cell K current was inhibited by external Ba and quinidine. Blockade by Ba was strongly voltage dependent, while that by quinidine was not. In the presence of high external Cl, a component of outward current that was inhibited by the anion channel blocker diphenylamine-2-carboxylate (DPC) appeared in 70% of the cells. This component was strongly outwardly rectifying and reversed at a potential expected for a Cl current. At the single channel level the event most frequently observed in the cell-attached configuration was a K channel with the following characteristics: inward-rectifying *I-V* relation with a conductance (with 112.5 mM K in the pipette) of 44 pS at the reversal potential, one open and at least two closed states, and open probability that increased with depolarization. Quinidine blocked by binding in the open state and decreasing mean open time. Several observations suggest that this channel is responsible for most of the whole-cell current observed in high external K, and for the K conductance of the basolateral membrane of the intact epithelium. On a few occasions a Cl channel was observed that activated upon excision and brief strong depolarization. The *I-V* relation exhibited strong outward rectification with a single channel conductance of 48 pS at 0 mV in symmetrical 112 mM Cl solutions. Kinetic analysis showed the presence of two open and at least two closed states. Open time constants and open probability increased markedly with

Address reprint requests to Dr. J. Fernando García-Díaz, Department of Physiology, Boston University School of Medicine, 80 East Concord Street, Boston, MA 02118.

J. GEN. PHYSIOL. © The Rockefeller University Press · 0022-1295/91/07/0131/31 $2.00
Volume 98 July 1991 131–161

depolarization. The similarity of the *I-V* relations of the single channel and the Cl-dependent component of whole-cell current suggests that the Cl channel is responsible for this component.

## INTRODUCTION

Since the pioneering work of Ussing (Ussing and Zerahn, 1951; Koefoed-Johnsen and Ussing, 1958), frog skin has been employed as a useful model for Na absorbing epithelia. There is a wealth of information on the transport properties and permeabilities of the apical and basolateral membranes of this epithelium, which has inspired work on other, less accessible, epithelial membranes. The apical membrane of the outermost living cell layer (*Stratum granulosum*) of the frog skin epithelium contains, almost exclusively, Na-selective amiloride-sensitive channels (Nagel, 1977). Cells in this layer are joined by tight junctions (Farquhar and Palade, 1964) maintaining the epithelial polarity. Cells from all epithelial layers are interconnected by intercellular junctions, forming a syncytium (Farquhar and Palade, 1964; Rick, Dörge, Arnim, and Thurau, 1978). The inner membrane of the *S. granulosum* and all membranes of the innermost layers contain Na-K ATPase (Farquhar and Palade, 1966; Mills, Ernst, and DiBona, 1977) and, presumably, the K channels that confer high K selectivity to the basolateral membrane. Na absorption involves an entry step through apical channels and an active extrusion from the cell by the Na-K ATPase in exchange for K uptake. K recycles through basolateral channels.

Although most transport modifiers act on apical Na channels, it is becoming clear that the basolateral membrane conductance is more labile than previously thought and may be involved in the regulation of salt and water absorption (Dawson and Richards, 1990). To elucidate the role of the basolateral conductance in Na absorption and in the maintenance of cell homeostasis it is crucial to characterize the ion transport mechanisms present at this membrane. This has proven elusive, however, mostly because of technical difficulties. Microelectrode studies have shown that most of the conductance of this membrane is due to K and it is partially inhibited by Ba (Nagel, 1979). No significant Cl conductance has been observed (Giráldez and Ferreira, 1984; Nagel, 1985), although it seems that a Cl conductance is activated during volume regulatory changes after cell swelling (Ussing, 1982). Noise analysis of the basolateral membrane has been hampered by the attenuating effect of the high resistance apical membrane (Van Driessche and Hillyard, 1985). Different approaches have been used to elucidate the *I-V* relation and conductance of the basolateral membrane, with results that do not generally agree (Nagel, 1985; Schoen and Erlij, 1985; Nagel, García-Díaz, and Essig, 1988). Such problems complicate the study of regulation of transport at this membrane and its possible relation with alterations in Na absorption.

In this paper patch-clamp techniques (Hamill, Marty, Neher, Sackman, and Sigworth, 1981) have been used to analyze the ionic conductances of enzymatically dissociated cells from frog skin epithelium. Since cells from all inner epithelial layers in frog skin contain membranes that are, from a functional point of view, basolateral, most dissociated cells will exhibit macroscopic properties identical to the basolateral membrane in the intact epithelium. The analysis of whole-cell and single channel currents confirmed this postulate. This approach allows a more detailed characteriza-

tion of the K and Cl conductive pathways at the basolateral membrane and provides a system where modification of K and Cl transport by regulatory agents can be directly studied.

A preliminary account of part of this work has appeared in abstract form (García-Díaz, 1990).

## MATERIALS AND METHODS

### *Chemicals and Solutions*

Amphibian culture medium (Wolf and Quimby, 1964), antibiotic-antimycotic mixture (100×, penicillin, streptomycin, and amphotericin B), and gentamicin sulfate (10 mg/ml) were obtained from Gibco (Grand Island, NY). *N*-Methyl-D-glucamine (NMDG) in base form and barium hydroxide were obtained from Fluka Chemical Corp. (Ronkonkoma, NY). Gluconate salts of these compounds were made by titration with D-gluconic acid (Sigma Chemical Co., St. Louis, MO). Tetramethylammonium (TMA) chloride was also obtained from Fluka Chemical Corp. Diphenylamine-2-carboxylate (DPC) was obtained from Pfaltz and Bauer Inc. (Waterbury, CT), nystatin (mycostatin) from Calbiochem Corp. (La Jolla, CA), and collagenase CLS-II from Worthington Biochemical Corp. (Freehold, NJ). All other chemicals were obtained from Sigma Chemical Co.

The NaCl Ringer solution contained 110 mM NaCl, 1 mM $CaCl_2$, and 2.5 mM KOH buffered to pH 7.6 with 4 mM HEPES. KCl, TMA Cl, Na gluconate, K gluconate, and NMDG gluconate solutions had the same composition except that NaCl was replaced by 110 mM of the corresponding salt. Ba was added either as $BaCl_2$ or Ba gluconate from a 1 or 0.5 M stock solution, respectively. Quinidine and DPC were added from 0.2 M stock solutions in dimethyl sulfoxide (DMSO). The pH of the DPC-containing Ringer was adjusted with 0.1 N NaOH. For recording single channel currents the pipette contained KCl Ringer, except in one case (Figs. 11 and 12) in which it contained NaCl Ringer. For measuring whole-cell currents the pipette contained 80 mM K gluconate, 20 mM KCl, 2 mM $MgCl_2$, 10 mM HEPES, 0.5 mM EGTA, and 4 mM $Na_2ATP$, buffered to pH 7.5 with KOH. During cell isolation the solution used (NaCl-AG) had the same composition as NaCl Ringer with the addition of 5 mM glucose, 1% antibiotic-antimycotic mixture and 0.5% gentamicin sulfate. The culture medium used contained 88.5% amphibian culture medium, 10% 0.15 M HEPES buffered to pH 7.6 with NaOH, 1% antibiotic-antimycotic mixture, and 0.5% gentamicin sulfate. All solutions were sterilized by filtration.

### *Cell Isolation*

Frogs (*R. pipiens* and *R. catesbiana*) were kept in an aquarium with access to running tap water and fed crickets. After double-pithing, the abdomen was scrubbed with a sterile gauze wetted with distilled sterilized water and a piece of abdominal skin was removed. All instruments used for isolation were presterilized and the procedures were carried out as aseptically as possible. The skin was incubated for 1 h at 18°C in NaCl-AG solution but with higher concentrations of antibiotic-antimycotic (10%) and gentamicin sulfate (1%). After rinsing in fresh unsupplemented NaCl-AG solution the epithelium was separated from the underlying dermis and connective tissue following a modification of the method of Fisher, Erlij, and Helman (1980). The internal surface of the skin was scraped with a scalpel to remove the tela subcutanea and the external surface was glued with tissue adhesive (Zipbond; Tescom Corp., Minneapolis, MN) to a piece of plastic film with a 14-mm-diam circular hole. The plastic film with the attached skin was placed, internal surface down, on top of a 35-mm Petri dish filled with a solution of collagenase (0.7 mg/ml) in NaCl-AG. The external surface was bathed with NaCl-AG and

covered to prevent drying. The collagenase solution was slowly agitated by a miniature magnetic stirrer. After 1.5 h the skin was rinsed with fresh NaCl-AG solution and the dermis was carefully removed with the use of fine forceps, while the epithelium remained attached to the plastic film. The epithelium covering the hole, which was not exposed to the adhesive, was rinsed again with NaCl-AG, cut into small pieces, and transferred to a 15-ml centrifuge tube containing trypsin (0.5 mg/ml, Sigma type III-S) in NaCl-AG. The pieces were incubated in trypsin for 30 min in a slow orbital mixer followed by mechanical disruption for 1 min by repetitive suction into a fire-polished Pasteur pipette. The resulting solution, containing dissociated cells as well as pieces of epithelium, was filtered through a mesh into another 15-ml centrifuge tube. The cells were washed twice by centrifugation and resuspension of the pellet into NaCl-AG containing 0.1% bovine serum albumin and one last time into NaCl-AG. After the final centrifugation the pellet was resuspended into 8 ml of culture medium and divided into four 35-mm tissue culture dishes (Falcon; Becton Dickinson and Co., Oxnard, CA). The dishes were kept in an incubator at a temperature of 18 ± 1°C and flushed with a mixture of 4% $CO_2$ in air. Cells kept for more than 48 h were refed by replacing half of the medium. Experiments were done on the day the cells were isolated and the following two days. Cell viability was tested by exclusion of trypan blue. A 0.1-ml aliquot of a 0.4% solution of trypan blue was added to 1 ml of the cell suspension, mixed, and added to the recording chamber. The coverslip bottom of the chamber had previously been treated with a 0.5% solution of concanavalin A in 1 M NaCl, rinsed with distilled water, and allowed to dry. After a few minutes to permit attachment of the cells to the bottom of the chamber, visual inspection revealed that >95% of the cells excluded the dye. By the third day the number of cells taking trypan blue started to increase. Cells stained with trypan blue did not attach well to the bottom of the chamber and were normally washed away after starting the superfusion. Those remaining retained the dye even after several hours of superfusion, thus ensuring that only viable cells were patched. The preparation appeared as a mixture of isolated, near-spherical cells of 10–30 μm diameter and of cell clusters. Only the larger cells (>20 μm) were patched. For whole-cell recordings only isolated cells were used.

In a few control experiments cells were dissociated by incubating the whole skin for 30 min in NaCl Ringer solution, without Ca and with 2 mM EGTA, followed by scraping of the apical surface and repetitive suction into a Pasteur pipette. This procedure produced few isolated cells and a considerable amount of debris. High-resistance seals were considerably harder to obtain and only single channel recordings were attempted. The results were similar to those obtained with cells isolated by the enzymatic procedure. No differences were observed in single channel or whole-cell currents between both species of frog and the results were pooled.

### *Electrical Measurements*

The recording chamber (with an approximate volume of 0.2 ml) was positioned on the stage of an inverted microscope (Nikon diaphot) with long working distance condenser and phase contrast optics. Solutions were superfused by gravity at a rate of 0.5 ml/min and changed by means of a six-way rotary valve (Rheodine 5011; Rainin Instrument Co., Woburn, MA). The bathing solution was connected to the reference electrode by a NaCl Ringer-4% agar bridge. Offset potentials were compensated by internal circuitry in the patch-clamp amplifier. Changes in liquid-junction potentials arising at the reference bridge when switching solutions were independently measured using a floating 3 M KCl junction and used to correct the results presented here. With reference to the NaCl Ringer the junction potentials were: −4 mV (KCl), 2 mV (TMA Cl), −11 mV (Na gluconate), −15 mV (K gluconate), and −5 mV (NMDG gluconate). In the cell-attached configuration the membrane patch voltage (cell-pipette) is given by $V_m = V_c - V_p$, where $V_c$ is the cell potential and $V_p$ the pipette voltage, both with reference to the bathing solution. When plotting current–voltage (*I-V*) relations in the

cell-attached configuration the voltage axis is plotted as $-V_p$. In this way depolarization of the patch corresponds to voltages to the right of the origin. In inside-out excised patches $V_m = -V_p$. Outward current is considered positive and plotted as upward deflection.

The headstage of the patch-clamp amplifier was mounted on a Huxley-type micromanipulator (Custom Medical Research Equipment, Glendora, NJ) at an angle of 45° with the horizontal. Pipettes were fabricated from 7052 Corning glass capillaries of 1.5 mm o.d. and 1.1 mm i.d. (Garner Glass, Claremont, CA) by two-stage pulling with a Kopf 730 puller (Tujunga, CA) to an outside diameter of 2.5 μm. The pipettes were bent at ~45° in a microforge so that when mounted on the holder and manipulator the tips were pointing down. The pipette tips were fire-polished to give a resistance of 8–18 MΩ in Ringer solutions.

Recordings were made with a patch-clamp amplifier designed and constructed by Dr. Enrico Nasi (Boston University School of Medicine, Boston, MA). The *I-V* converter amplifier was a low noise Burr-Brown OPA 101 (Tucson, AZ) with switchable feedback resistors of 50 GΩ and 100 MΩ. The instrument provided capacitance compensation with three time constants, series resistance compensation, and 4-pole Bessel filter. With the input open, the noise level was 0.17 pA p–p at 1 kHz. Currents were monitored on a digital storage oscilloscope (model 310; Nicolet Instrument Corp., Madison, WI). Single channel currents were filtered at 1 or 2 kHz and stored on video tape with a modified pulse code modulator (Toshiba DX-900; model DAS 900; Dagan Corp., Minneapolis, MN). They were later sampled at five times the filter frequency and stored in computer files for analysis. Single channel currents shown in the figures were played back into a Gould Inc. (Cleveland, OH) strip-chart recorder (corner frequency ~90 Hz) at 1/10 the original speed. Whole-cell currents were digitized and stored in an IBM AT computer equipped with DT 2821 AD/DA board (Data Translation Inc., Marlborough, MA). The software for data acquisition and analysis of whole-cell and single channel currents was developed by Dr. Enrico Nasi. The kinetic analysis was done with records containing only a single channel. Opening and closing transitions were determined by setting a half-amplitude threshold. The records analyzed were of variable duration but they contained a minimum of 1,000 crossings. Open and closed time distributions were fitted to exponentials using a Simplex algorithm.

High-resistance seals (> 10 GΩ) were obtained after applying stable suction, controlled by a miniature vacuum regulator (Air Trol V-4104; Minuteman Controls, Wakefield, MA), to the pipette. In initial whole-cell recordings the patch was ruptured by applying higher suction and 4-ms pulses of −200 mV. In subsequent experiments, the perforated patch technique of Horn and Marty (1988) was used. The pipette tips were filled, up to 0.8–1 mm, with intracellular solution while the rest of the pipette was back-filled with the same solution containing 250 μg/ml nystatin. A stock solution of 50 mg/ml nystatin in DMSO was prepared fresh before the experiment by vortexing and sonication and kept in the dark. After the formation of a GΩ seal the fast current transient due to the electrode capacitance was compensated. After 20–30 min a large transient became apparent, indicating insertion of nystatin into the patch membrane and charging of cell capacitance. After an additional 5 min the capacitive transient reached a maximum value. Analysis of the transient (with the filter set at 10 kHz) showed that it could be fitted with a single exponential. Values of cell capacitance obtained by this method were in the range 14–32 pF, in reasonable agreement with cell sizes of 20–30 μm diameter. Cell resistances ranged from 1 to 3.5 GΩ in NaCl Ringer. Access resistances were two to four times the electrode resistance and they were partially compensated. The capacitative transients were also compensated before recording.

Pulses were applied with a digital stimulator (Stim 6; DAQ, Milton, MA). Seal formation was monitored with a −10-mV pulse of 40 ms applied every 200 ms. Whole-cell currents were elicited by pulses of 100 or 200 ms duration every 3 or 5 s, ranging from −140 or −160 mV to 60 or 100 mV, in 20-mV steps, from a holding potential of −60 mV. Because the currents did

not show any time-dependent kinetics, they were subsequently elicited by applying a voltage ramp from −140 to 100 mV at a rate of 100 mV/s using a model 184 generator (Wavetek, San Diego, CA). At this rate, assuming a maximum cell capacitance of 50 pF, the capacitive current would be only 5 pA. Five consecutive ramps in each experimental condition were averaged on-line and stored on disk. Analogue leak subtraction was not possible since channels were active at all voltages (see Results). Average values are given as mean ± SD.

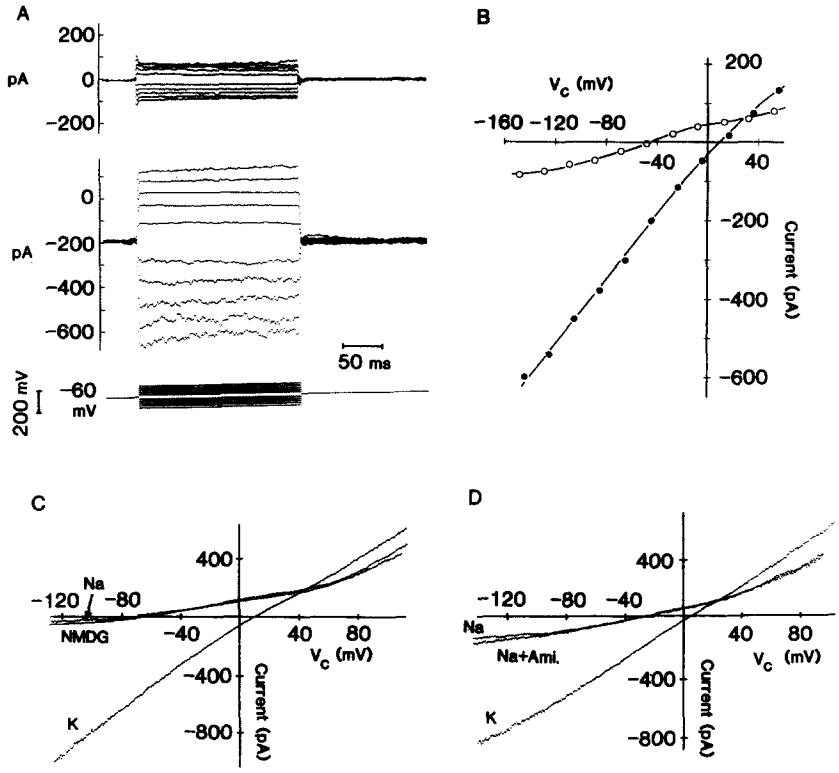


FIGURE 1. Cation dependence of whole-cell currents. (*A*) Whole-cell currents in response to voltage pulses with Na gluconate Ringer (*top traces*) or K gluconate (*middle traces*) in the bath. Voltage pulses from −60 to −140 and to +60 mV and 200 ms duration are shown by the bottom traces. (*B*) *I-V* relation for the currents shown in *A* with Na ( *open circles*) or K (*filled circles*) in the bath. (*C*) Whole-cell currents from a different cell in response to a voltage ramp with Na, NMDG, or K gluconate solutions in the bath. (*D*) Whole-cell currents from a different cell in response to a voltage ramp with Na, Na plus 20 μM amiloride, or K gluconate solutions in the bath.

## RESULTS

### *Whole-Cell Currents*

Fig. 1 *A* shows the currents recorded in Na (top) and K (middle) with gluconate as the main anion. Whole-cell currents showed no consistent time dependent kinetics in any bathing solution used. After substituting K for Na two major effects are evident: the

baseline current, which at the holding voltage of −60 mV was near zero, becomes near −200 pA while the cell conductance increases. Fig. 1 *B* shows the *I-V* relation for values taken 160 ms after the onset of the pulse. The reversal potentials were in the range −30 to −83 mV in Na medium (see below). After substitution the reversal potential shifted toward more positive values (see Fig. 1), as expected for a cell membrane with a high K conductance. In K medium the average reversal potential was 10 ± 5 mV ($n$ = 19).[1]

The variability in reversal potentials in Na medium among experiments (compare Fig. 1, *C* and *D*) was in part due to the presence of leak (see Discussion). This prevented the calculation of a relative Na/K permeability. To test for a Na component of inward current the bathing solution was changed to one with NMDG as the main cation. Fig. 1 *C* shows the currents recorded in these different solutions using the ramp protocol described in Methods. In all cells tested there was no significant difference between currents recorded with Na or NMDG as main bath cations. In three experiments such as that shown in Fig. 1 *D*, 20 μM amiloride was added to the Na medium without a significant change in the currents. These observations indicate that there is little, if any, Na component in the currents and that K is the main charge carrier. The crossover of outward currents shown in Fig. 1, *B–D*, is of significance since it indicates a stimulation of K efflux by high external K, suggesting, as discussed later, a multi-ion permeation mechanism where independence of ion fluxes is not obeyed (Hille and Schwarz, 1978). The *I-V* relations in K gluconate were near linear or with a slight inward rectification (Figs. 1–3). At the reversal potential the conductance was 5 ± 3 nS ($n$ = 19).

Further evidence for the notion that K is the ion responsible for the observed currents is provided by blockade by Ba. Fig. 2 *A* shows the currents in K gluconate before (top) and after (middle) the addition of 5 mM $BaCl_2$. In the presence of Ba the baseline current (at the holding voltage of −60 mV) decreases while the response to hyperpolarizing pulses is also smaller than the baseline. This is clearly seen in the *I-V* relations (Fig. 2 *B*) showing the strong voltage dependence of Ba blockade. Another experiment, this time with the ramp protocol and using Ba gluconate, is shown in Fig. 2 *C*. The inhibition by Ba was reversible after 5–10 min. The effects observed were the same independent of whether Cl or gluconate salts of Ba were used. To analyze the voltage dependence of Ba blockade the ratio of currents in the presence and absence of Ba ($I_{Ba}/I$) were plotted against the cell potential (Fig. 2 *D*, filled circles). For a one-to-one reaction of the type Ba + R = RBa, where R is the receptor or site where Ba binds, the current ratio is expected to follow the relation (Standen and Stanfield, 1978; Latorre and Miller, 1983; Moczydlowski, 1986):

$$I_{Ba}/I = 1/\{1 + ([Ba]/K_d(0)) \exp(-z\delta FV_c/RT)\} \quad (1)$$

where [Ba] is the Ba concentration, $K_d(0)$ is the dissociation constant at zero voltage, $z$ is the valence of Ba (+2), $\delta$ is the fraction of the electrical field at the binding site,

[1]This value is probably some 8–12 mV more positive than the actual reversal potential because the offset potentials of the pipettes filled with intracellular solution were cancelled with the tips immersed in NaCl medium. This offset includes then a liquid junction potential, which, after equilibration with the cell interior, is mostly dissipated.

and the other symbols have their usual meaning. The data were fitted to the above equation using a Marquardt-Levenberg curve fitting algorithm. The resulting function is shown by the solid line in Fig. 2 *D*. The average values of $\delta$ and $K_d(0)$ for eight experiments were 0.3 ± 0.1 and 27 ± 21 mM, respectively. In some instances, the data points did not fit well with Eq. 1 because (*a*) the inhibition was less than expected at negative voltages, and (*b*) there was inhibition even at large positive

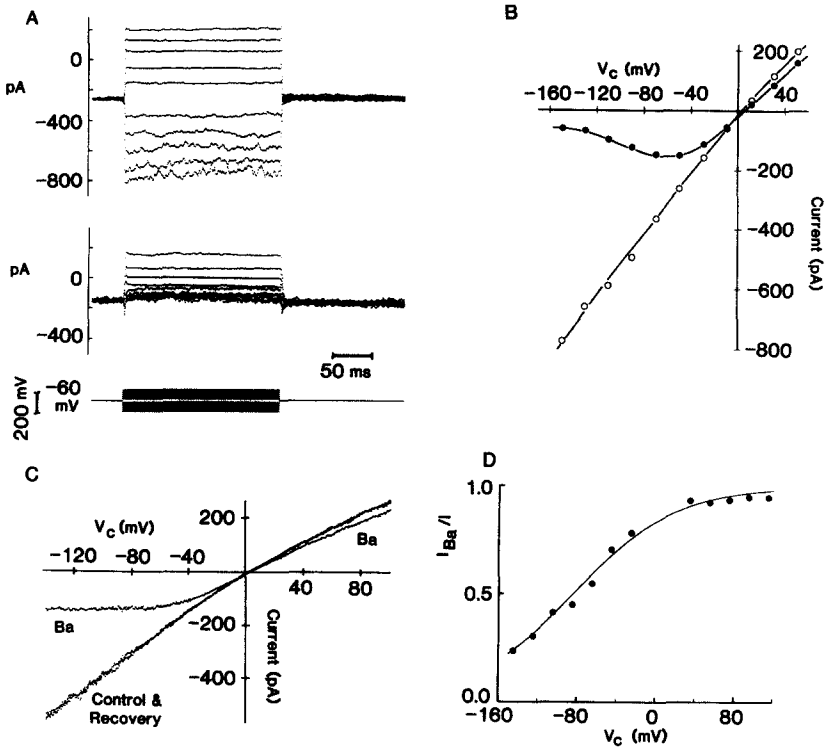


FIGURE 2. Blockade by Ba of whole-cell currents. (*A*) Whole-cell currents in response to voltage pulses in the absence (*top traces*) and presence (*middle traces*) of 5 mM $BaCl_2$. Bath solution was K gluconate. Voltage pulses (*bottom traces*) were as in Fig. 1. (*B*) *I-V* relation for the currents in *A* in the absence (*open circles*) and presence (*filled circles*) of Ba. (*C*) Whole-cell currents in a different cell in response to a voltage ramp before, during, and after addition of 5 mM Ba gluconate to the bath. (*D*) Ratio of currents in presence and absence of Ba ($I_{Ba}/I$) versus cell potential (*filled circles*). For voltages in the range 0 ± 20 mV the error in the calculation of the current ratios was large and the data were omitted from the figure. The continuous line was obtained by fitting the values to a Boltzmann relation (see text).

voltages. This last effect is seen in Fig. 2, *B* and *C*. Probable causes for these deviations are considered in the Discussion.

Quinidine added to the extracellular solution also inhibited the K currents. Unlike Ba, however, quinidine blockade was mostly voltage independent (Fig. 3 *A*). The ratio of currents in the presence and absence of quinidine was approximately constant in the range −140–40 mV for each concentration of quinidine tested (Fig. 3 *B*). There

was a slight relief of block at voltages more positive than 40 mV. Blockade by quinidine was reversible after ~15 min.

The experiments described above were done with gluconate as the main anion in the external solution. It was important to ascertain the presence of a Cl component in the whole-cell currents, particularly since there may be a basolateral Cl conductance in epithelial cells of frog skin that is activated under certain conditions (Ussing, 1982, 1986). With Na as the main cation outward currents were larger in the presence of high external Cl than with gluconate (Fig. 4 *A*, top and middle). The *I-V* relations (Fig. 4 *B*) clearly show the increase in outward current in high external Cl, without a significant change in reversal potential. The effect of high external Cl was reversible and was observed in eight cells, while in three others the substitution of Cl for gluconate did not have any significant effect. To test whether the increase in outward current is due to an influx of Cl rather than a stimulation of K efflux, the effect of the Cl channel blocker diphenylamine-2-carboxylate (DPC) (Di Stefano, Wittner, Schlat-

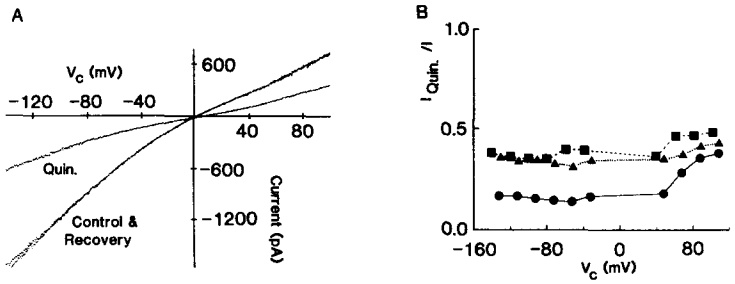


FIGURE 3. Inhibition of whole-cell currents by quinidine. (*A*) Whole-cell currents in response to a voltage ramp before, during, and after exposure to 0.5 mM quinidine. Bath solution was K gluconate. (*B*) Ratio of currents in the presence and absence of quinidine ($I_{Quin}/I$) versus cell potential. Three different experiments with different quinidine concentrations (▲, 0.1 mM; ■, 0.5 mM; ●, 1.0 mM) are shown. For voltages in the range 0 ± 20 mV, the error in the calculation of the current ratios was large and the data were omitted from the figure.

ter, Lang, Englert, and Greger, 1985; Welsh, 1986*b*) was investigated. As shown in Fig. 4 *C*, DPC at 1 mM reversibly inhibited the outward current present with high external Cl. Assuming that DPC only affects the Cl current component (see Discussion), this will be given by the difference between the currents in the absence and presence of the blocker (Fig. 4 *D*). The Cl current exhibited a strong outward rectification with a reversal potential of −41 ± 4 mV ($n$ = 3), in agreement with the calculated Cl equilibrium potential of −39 mV.

*Single Channel Currents*

Cell-attached single channel currents were recorded with patch pipettes filled with KCl Ringer solution. On average only ~10% of the patches contained active channels. With NaCl Ringer in the bath, the event most often observed was an inward current of amplitude −3.8 ± 1.3 pA ($n$ = 14) at zero pipette voltage. Fig. 5 shows current records at several pipette voltages from a patch containing a single channel

of this type. For all the records shown the current was inward, increasing in amplitude with hyperpolarization ($V_p > 0$). The *I-V* relation for the same experiment is shown in Fig. 6*A*. The single channel conductance at $V_p = 0$ was 80 pS. At this voltage the average conductance for 14 experiments was 73 ± 10 pS. The single channel current in Fig. 6*A* reversed at a $V_p$ of −89 mV. Reversal potentials were

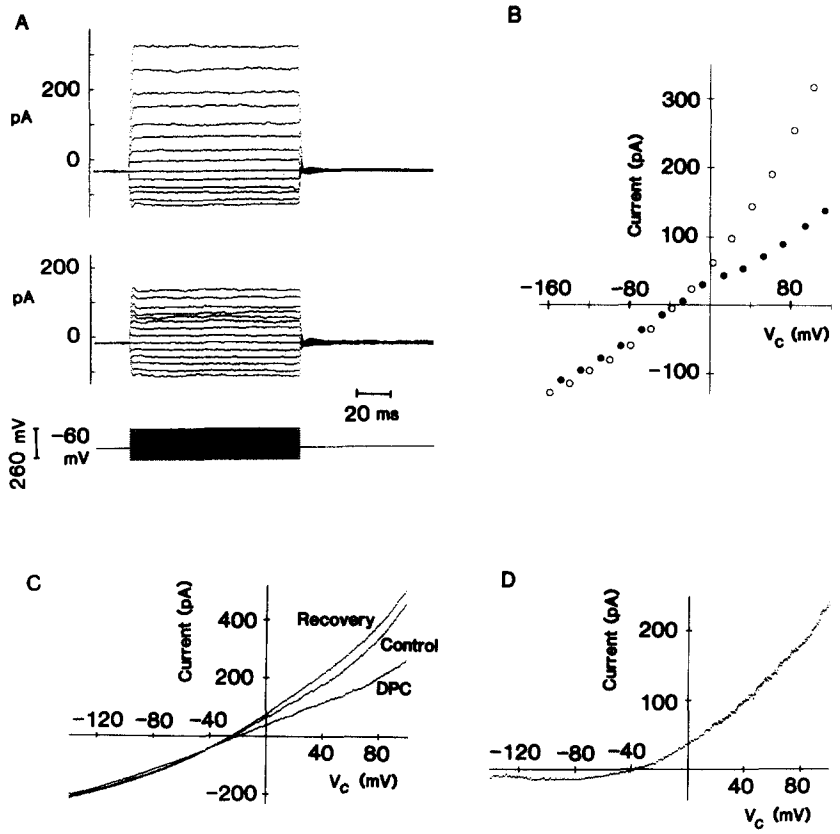


FIGURE 4. Anion dependence of whole-cell currents. (*A*) Whole-cell currents in response to voltage pulses with NaCl Ringer (*top traces*) or Na gluconate (*middle traces*) in the bath. The voltage pulses from −60 to −160 and to +100 mV and 100 ms duration are shown in the bottom traces. (*B*) *IV* relation for the currents in *A* with Cl (*open circles*) or gluconate (*filled circles*) as the main anion in the bath. (*C*) Whole-cell currents in response to a voltage ramp before, during, and after exposure to 1 mM diphenylamine-2-carboxylate (DPC). Bath solution was NaCl Ringer. (*D*) Difference between currents after and during DPC treatment for the experiment shown in *C*.

variable among experiments (range −40 to −89 mV, average −67 ± 15 mV, $n = 14$), although they were similar for cells from the same preparation. With K and Cl as the major ions in the pipette, the unitary current must be carried by either one of these ions. Since the concentrations of K in the pipette and the cell are similar (García-Díaz, Baxendale, Klemperer, and Essig, 1985) a current carried by K should reverse

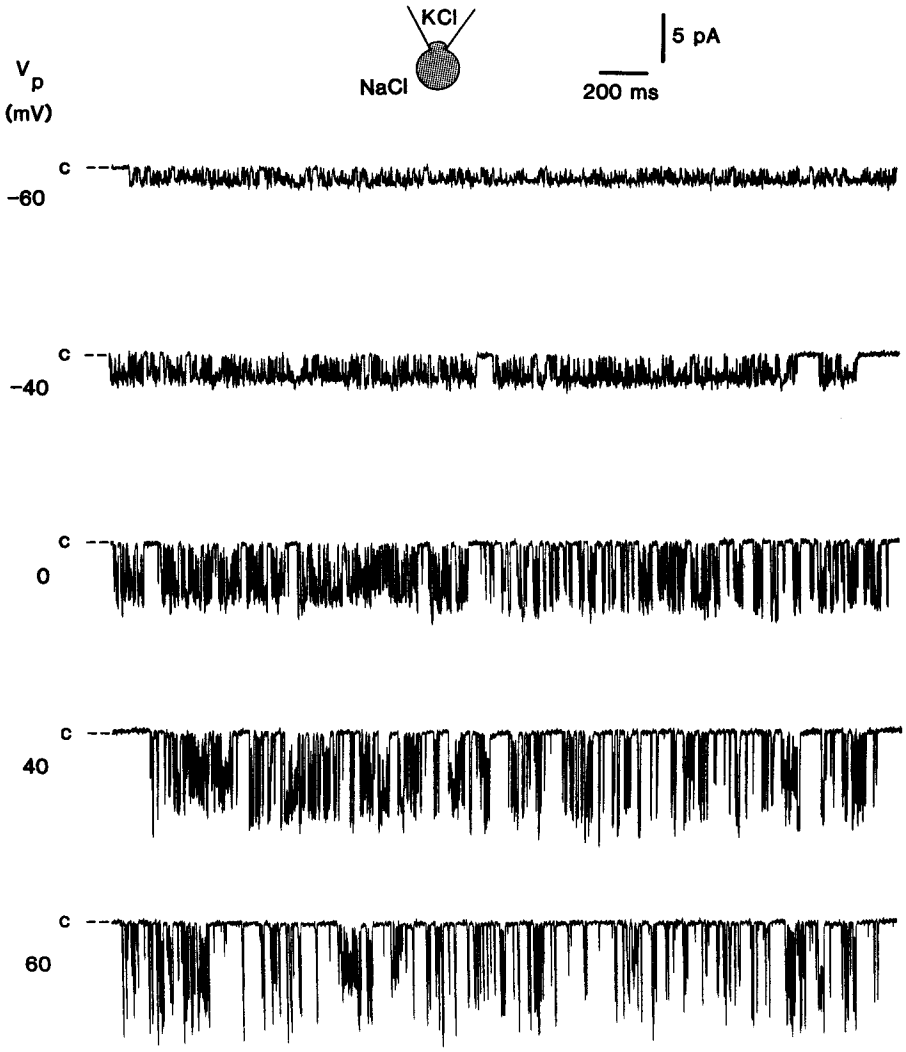


FIGURE 5. Cell-attached single channel currents recorded at different pipette voltages. Pipette and bath contained KCl and NaCl Ringer solutions, respectively. Zero current levels are indicated by the lines marked *C* on the left side. All currents shown are inward (pipette to cell). Records were filtered at 2 kHz, sampled at 10 kHz, and played back to the stripchart recorder at 1/10 the original speed.

at a pipette voltage ($V_p$) equal to the cell potential ($V_c$). On the other hand, estimates of intracellular Cl activities (Nagel, García-Díaz, and Armstrong, 1981; Giráldez and Ferreira, 1984) indicate that for a Cl current the reversal should occur at a $V_p$ some 38 mV more positive than $V_c$. Although the actual values of $V_c$ for these experiments were not measured, they are likely to be near the observed reversal potentials (García-Díaz et al., 1985), suggesting that K is the major ion crossing this channel.

Other evidence described later supports this conclusion. The selectivity of the channel could not be measured since activity disappeared on excision of the patch.

To account for the variability in reversal potentials ($V_p^{rev}$) the *I-V* relations were normalized by shifting $V_p$ by $V_p^{rev}$ in Fig. 6 *B*, which shows data from 14 experiments. If the reversal potential is equal to the cell potential, the abscissa represents the actual voltage across the membrane patch ($V_m = V_c - V_p$ ). As shown by the figure, the *I-V* relations exhibited inward rectification. At the reversal potential the average single channel conductance was 44 pS.

As shown in Fig. 5, opening of the channel occurred in bursts separated by silent periods of up to several hundred milliseconds, which became more frequent with hyperpolarization of the patch. In general the probability of finding the channel open decreased with hyperpolarization. Fig. 7 shows amplitude histograms and open time distributions at three different voltages for the experiment of Fig. 5. Only two current levels, corresponding to the closed and open conductive states of the

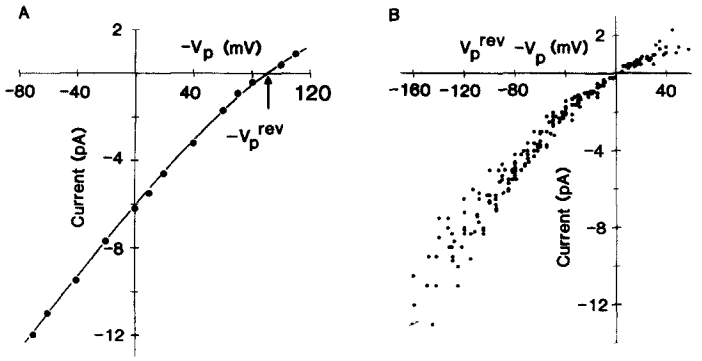


FIGURE 6. Single channel *I-V* relations. Note that the voltage axis is the negative of the pipette potential. (*A*) *I-V* relation for the experiment of Fig. 5. Reversal potential ($V_p^{rev}$) was −89 mV. (*B*) *I-V* relations for 14 experiments. The voltage was shifted by the value of $V_p^{rev}$ for each experiment.

channel, were present. The relative number of open events decreased with hyperpolarization. The open time distributions for this experiment were fitted by single exponentials, as was the case for 10 of 12 experiments, giving an average value of the open time constant of $\tau_0 = 8.1 \pm 4.5$ ms at $V_p = 0$. In the other two experiments an additional exponential with a shorter time constant was required. Fig. 7 also shows that the mean open time for this channel decreased with hyperpolarization. Analysis of the closed-time distributions was restricted to short closed times (inside bursts) as the records sampled were not long enough to contain a sufficient number of the longer shut periods. For the experiment of Figs. 5 and 7 the closed-time distributions could be fitted to single exponentials (not shown) with time constants ($\tau_c$) of 2.1 ms ($V_p = -40$ mV), 2.6 ms (0 mV), and 3.3 ms (40 mV). Thus, the closed time constant increased with hyperpolarization. In 9 of 12 experiments the closed-time distributions at $V_p = 0$ could be fitted with a single exponential of $\tau_c = 1.6 \pm 0.7$ ms. The other three required an additional exponential with longer time constant. The voltage dependencies of $\tau_0$, $\tau_c$, and fractional open time (*f*, open time probability) are

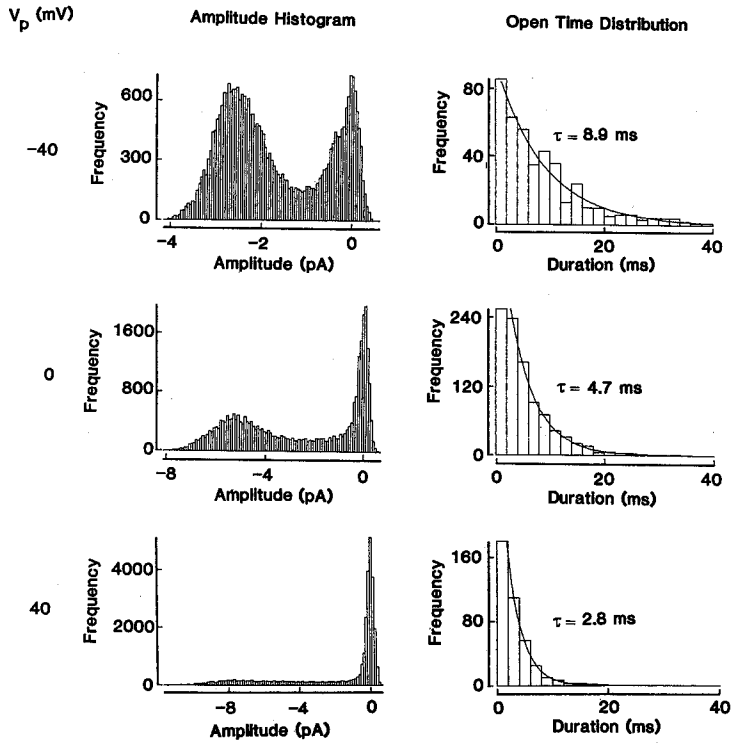


FIGURE 7. Amplitude histograms (*left*) and open-time distributions (*right*) at three different voltages for the single channel shown in Fig. 5. The open-time distributions were fitted with single exponentials with time constants indicated in the figure.

shown in Fig. 8 for four experiments where long enough records at several voltages were obtained. There was some variability among experiments, although in general $f$ increased with depolarization while $\tau_c$ decreased slightly. In two experiments the open time constant showed a strong increase with depolarization, as was the case for the experiment in Fig. 7, but it hardly changed in two other cases.

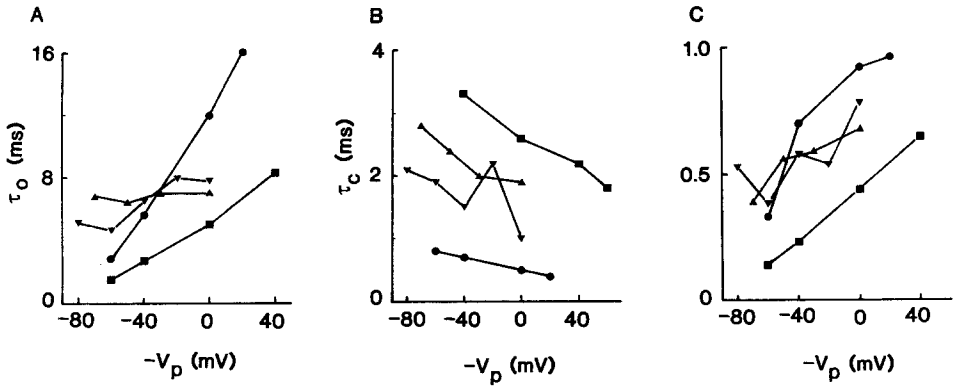


FIGURE 8. Voltage dependence of open (*A*) and closed (*B*) time constants and fractional open time (*C*) for four different experiments. Lines join points from the same experiment.

To establish more clearly the nature of the K selectivity of the channel the cells were depolarized by changing the bath to KCl Ringer. This removes the uncertainty in the value of $V_c$, and if the channel is K-selective the single channel current should reverse near $V_p$ = 0 mV. Fig. 9 *A* shows a single channel current record at a $V_p$ of 0 mV. At the time marked by the vertical arrow the bath was changed to high K. The

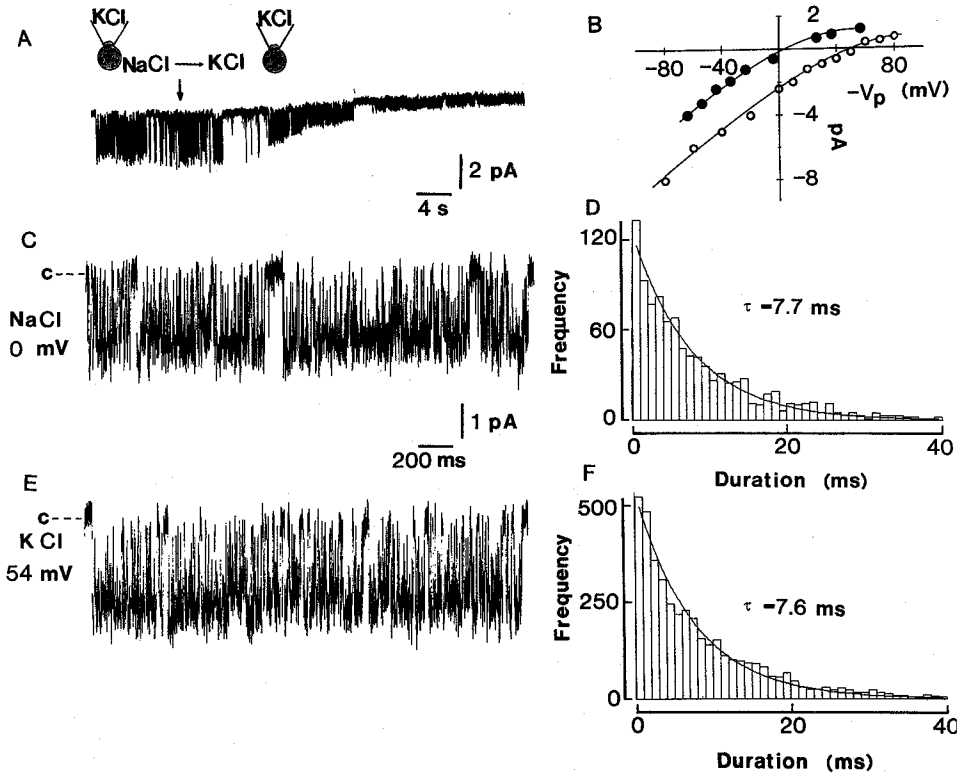


FIGURE 9. Effects on single channel currents of substitution of K for Na. (*A*) Cell-attached single channel currents recorded with KCl Ringer in the pipette at a voltage of 0 mV. At the time marked by the vertical arrow the bath solution was changed from NaCl to KCl Ringer. The shift in baseline is due to the appearance of a 4-mV junction potential at the reference bridge and the relatively low seal resistance in this experiment. (*B*) Single channel *I-V* relations for the experiment shown in *A*, with NaCl (*open circles*) and KCl (*filled circles*) in the bath. (*C*) Single channel currents recorded with NaCl in the bath at 0 mV. (*E*) Single channel currents from the same cell with KCl in the bath at a pipette voltage of 54 mV. (*D* and *F*) Open time distributions for the records shown in *C* and *E*. In both cases the distributions were fitted with single exponentials of similar time constants.

amplitude of the inward current gradually declined from 2.3 pA to a value of $<0.5$ pA. The *I-V* relations in Na and K media are shown in Fig. 9 *B*. The reversal potential shifted from $-53$ to $-3$ mV after the substitution. In six experiments the average reversal potential with KCl Ringer in the bath was $-5 \pm 6$ mV. These experiments support the notion that the channel current is carried by K. Current through a

Cl-selective channel would reverse at a pipette potential of 38 mV. The kinetics of the channel was not altered by the presence of high extracellular K, other than by the shift in potential across the patch. Fig. 9, *C* and *E*, show single channel records in NaCl at $V_p = 0$ and in KCl at $V_p = 54$ mV. This potential was chosen to give a similar current amplitude to that in NaCl with $V_p = 0$. The open time distributions for each situation are shown in Fig. 9, *D* and *F*. Both distributions could be fitted with single exponentials of similar time constants.

Since the channel activity disappeared on excision and its kinetics varied considerably from cell to cell, blockage was investigated with the permeant inhibitor quinidine. Fig. 10 shows the effect of quinidine on the single channel currents. The bath solution was KCl Ringer to depolarize the cell potential and minimize the effect of quinidine on $V_c$. The pipette potential was held at −56 mV. Under these conditions the current is outward and the channel stays mostly open (Fig. 10, top trace). The bottom trace was obtained 2 min after the addition of 0.1 mM quinidine to the bath. There was a slight decrease (~10%) in the current amplitude at this voltage. This small decrease was not seen at all potentials and it probably reflects changes in $V_c$ induced by quinidine. Channel kinetics was markedly affected by quinidine. In the control state the open and closed time distributions (Fig. 10, left) were reasonably well fitted by single exponentials with $\tau_0 = 23$ ms and $\tau_c = 1.2$ ms, respectively. A longer closed state is not apparent in the distribution since there were few of these events in the records analyzed. Addition of quinidine reduced $\tau_0$ by a factor of 10, to 2.2 ms, and the closed time distributions now exhibited two different time constants, a short one of 1.4 ms, similar to that found in the absence of the blocker, plus a long one of 50 ms which was not present before addition of quinidine. These results are consistent with a model of blockade in which the blocker binds to the channel only in the open state (Colquhoun and Hawkes, 1983; Moczydlowski, 1986):

$$C \underset{\alpha}{\overset{\beta}{\rightleftharpoons}} O \underset{k_{off}}{\overset{k_{on}[Q]}{\rightleftharpoons}} B \qquad (2)$$

where $\alpha$, $\beta$, $k_{on}$, and $k_{off}$ are the rate constants, and [Q] the quinidine concentration. As indicated above, the kinetics of the unblocked channel is complex, with at least two different closed states. However, by recording at depolarized potentials the number of long closed states is reduced and their influence in the distributions minimized, so that it is possible to describe approximately the kinetics with only single open and closed states. The mean open time is given by the inverse of the sum of the rates of the reaction paths leaving the open state. For the sequential model of reaction (Eq. 2) the mean open time in the absence of quinidine is $1/\alpha$, while addition of quinidine will shorten the mean open time to $1/(\alpha + k_{on}[Q])$. The model predicts also that a blocked state with a mean dwell time of $1/k_{off}$ will appear in addition to the closed state, in agreement with the experimental results.

A different channel was observed on a few occasions, mostly after excision of the patch. Fig. 11 shows single channel current records of such an excised patch. Before excision this patch did not show any channel activity. After excision the channel was activated by briefly depolarizing the patch by 200 mV. The ionic selectivity of this channel was studied by changing the bath solutions. Fig. 12 *A* shows the *I-V* relation

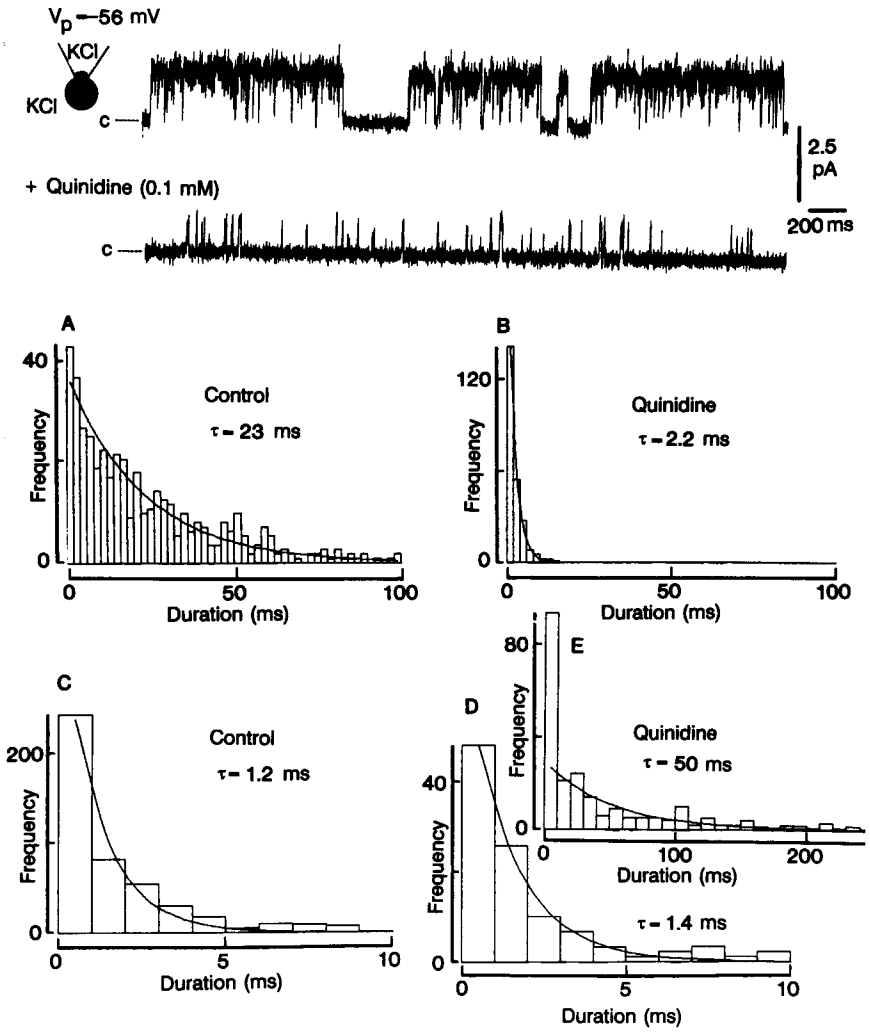


FIGURE 10. Effect of quinidine on single K channel currents. The top record shows the single channel current obtained with KCl Ringer in bath and pipette at a pipette potential of −56 mV. Under these conditions the current is outward. The baseline (zero current level) is indicated by *C* on the left. The next record is from the same experiment 2 min after exposure to 0.1 mM quinidine. Open- and closed-time distributions are shown for the control period (*A* and *C*) and for records obtained after addition of quinidine (*B*, *D*, and *E*). For the analysis of the closed times in the presence of quinidine the cumulative distribution up to 10 ms was analyzed first, with bin sizes of 1 ms. Then the bin size was increased to 10 ms and the distribution was fitted with an exponential up to 240 ms, starting with the second bin. In the absence of quinidine there were < 10 closed events longer than 10 ms.

for the channel of Fig. 11, both with NaCl and TMA Cl solutions in the bath and NaCl Ringer in the pipette. The *I-V* relations were the same in both solutions, with a pronounced outward rectification. Fig. 12 *B* shows the *I-V* relations for another experiment where the pipette contained KCl and the bath was changed from NaCl to

KCl and to Na gluconate. There was a significant shift in the reversal potential towards negative values after substituting bath Cl with gluconate. This indicates that the channel is Cl selective. Assuming negligible cation permeability (substitution of the large cation TMA for Na did not affect the *I-V* relation, Fig. 12 *A*), the permeability ratio $P_{Cl}/P_{gluc}$ can be calculated from the shift in reversal potential in Fig. 12 *B*. For this experiment $P_{Cl}/P_{gluc}$ was 9, while in a different experiment it was 34.

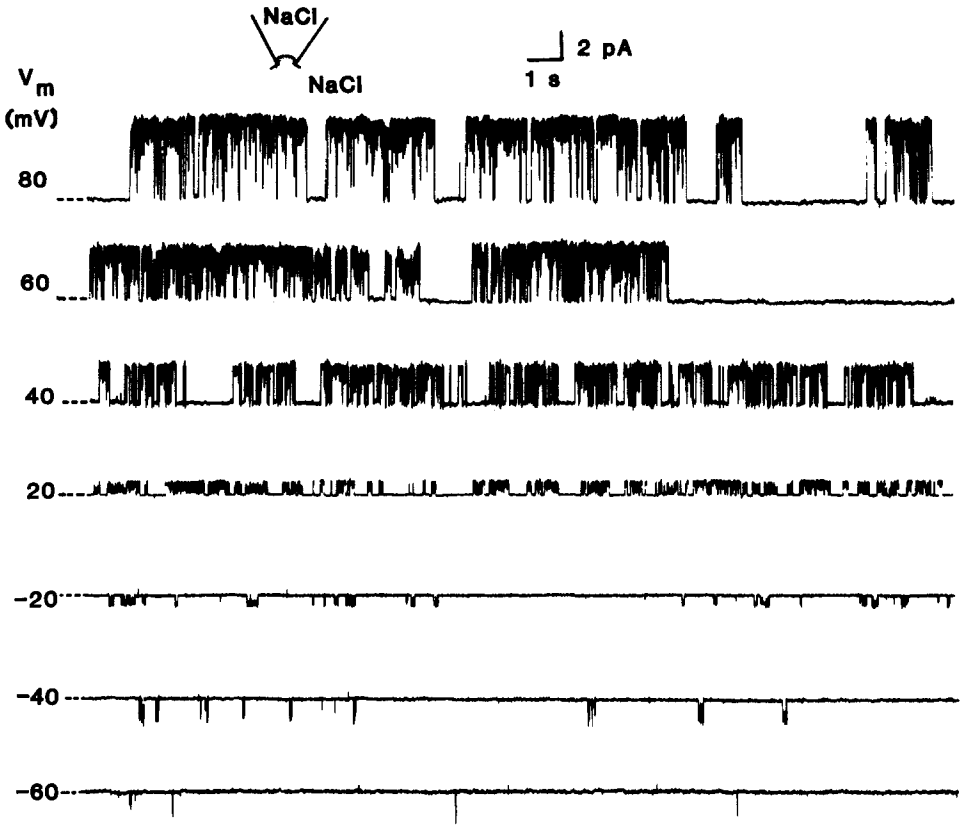


FIGURE 11. Single channel currents recorded from an excised patch (inside out) with NaCl Ringer in pipette and bath. Membrane patch (bath-pipette) voltages are shown at the left of each trace. The baseline (zero current level) is indicated by the dashed lines at the left of each record. The currents were filtered at 0.5 kHz, sampled at 2.5 kHz, and played back into the stripchart recorder at the original speed.

With symmetrical 112 mM Cl solutions the single channel conductance was 48 ± 3 pS ($n$ = 4) at 0 mV and increased to 76 ± 7 pS at 50 mV.

As shown in Fig. 11, the Cl-selective channel opened in bursts separated by long shut periods. The duration of these shut periods increased with hyperpolarization. Fig. 13 shows the kinetic analysis for this channel. At the top are the amplitude histogram and open- and closed-time distributions obtained at 60 mV. The amplitude histogram shows that only two current levels were present. The open-time

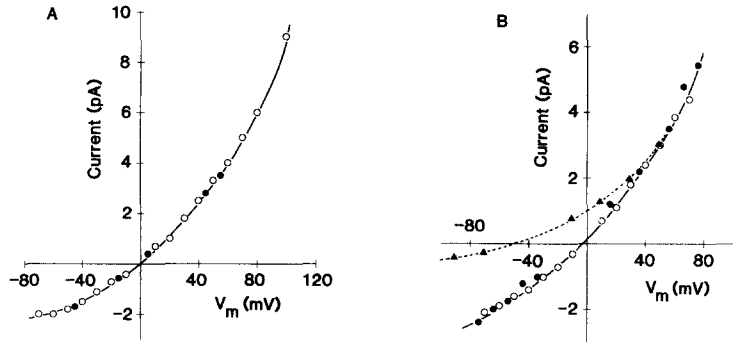


FIGURE 12. Excised (inside out) single channel *I-V* relations. (*A*) *I-V* relations for the channel of Fig. 11 with NaCl in the pipette and NaCl (*open circles*) and TMA Cl (*filled circles*) in the bath. (*B*) *I-V* relations from a different experiment with KCl in the pipette and NaCl (*open circles*), KCl (*filled circles*), or Na gluconate (*filled triangles*) as bath solutions.

distribution required two exponentials for fitting, while the closed times were fitted with only a single exponential with a time constant of 1.1 ms. It is clear from the records in Fig. 11, however, that at least one long closed state is also present, but the number of such events was small during the periods recorded. Thus, this channel apparently has two open and no less than two closed states. The voltage dependence

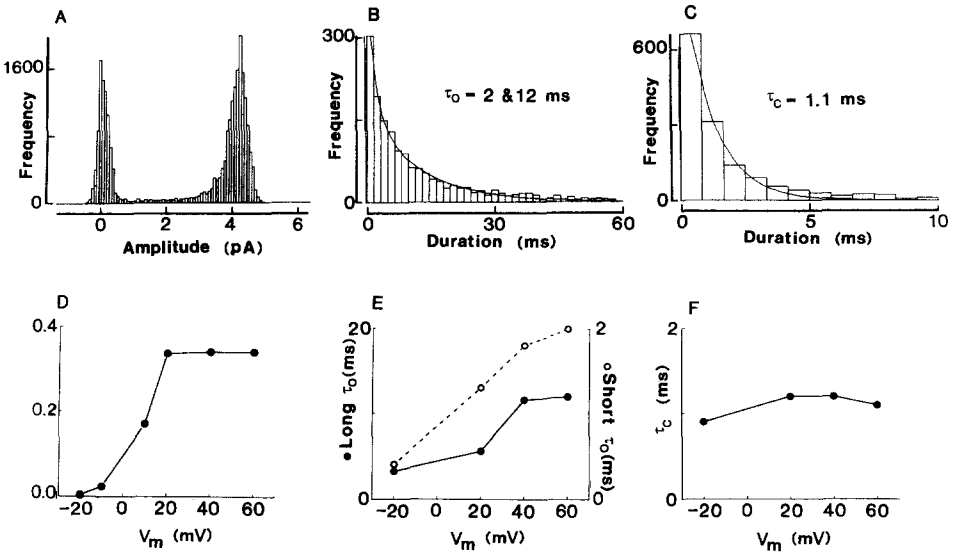


FIGURE 13. Amplitude histogram (*A*) and open- (*B*) and closed-time (*C*) distributions for the Cl channel of Fig. 11 at a voltage of +60 mV in the excised configuration. The open-time distribution was fitted by the sum of two exponentials of time constants 2 and 12 ms. The closed-time distribution required only one exponential with a time constant of 1.1 ms. *Bottom*, voltage dependence of the fractional open time (*D*) and open (*E*) and closed (*F*) time constants for the same experiment.

of the fractional open time and of the open and closed time constants are shown in the bottom graphs of Fig. 13. These include only those voltages at which there were records with a sufficient number of crossings to give meaningful exponential fittings of the distributions. The fractional open time was strongly voltage dependent,

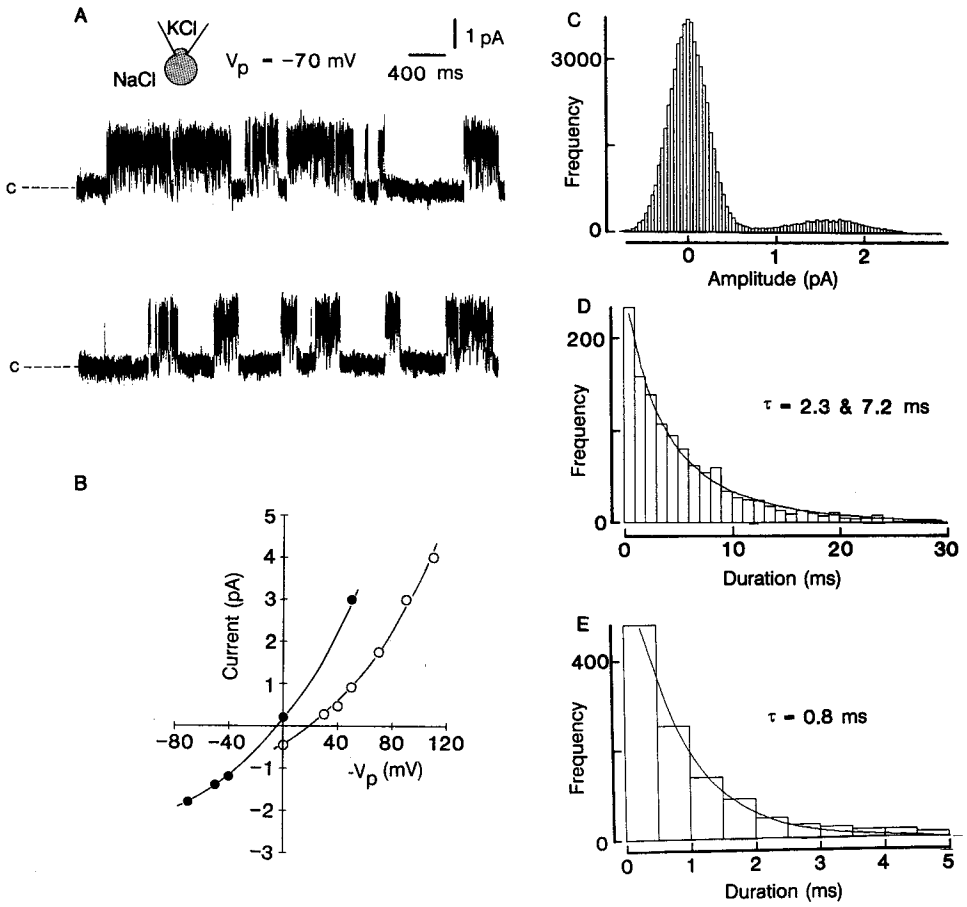


FIGURE 14. Single Cl channel currents recorded in the cell-attached configuration. (*A*) Continuous current records obtained with KCl in the pipette and NaCl Ringer in the bath at a pipette voltage of −70 mV. At this voltage the current is outward. The baseline is indicated by the line marked *C*. (*B*) *I-V* relations for the same experiment shown in *A* in the cell-attached mode (*open circles*) and after excision of the patch (*filled circles*). *C, D,* and *E:* Amplitude histogram and open- and closed-time distributions, respectively, for the currents recorded in the cell-attached configuration at −70 mV.

increasing *e*-fold for 6.7 mV depolarization. Both open time constants, short and long, increased with depolarization, while the closed time constant was insensitive to voltage. Much of the strong voltage dependence of $f$ seems to be due to the long shut periods between bursts.

As indicated, the Cl channel was rarely seen in the cell-attached configuration. One such experiment is shown in Fig. 14. The top records (Fig. 14 *A*) are single channel currents at $V_p = -70$ mV with NaCl in the bath and KCl in the pipette. The *I-V* relations for this channel before (Fig. 14, open circles) and after excision (Fig. 14, filled circles) are shown in *B*. Note that in the cell-attached mode the reversal potential was −22 mV, which is consistent with the Cl selectivity of the channel. Fig. 14, *C–E,* show the amplitude histogram and open- and closed-time distributions for the on-cell recording. As observed in the excised mode, the open-time distribution required two exponentials for fitting, while only one exponential with a short time constant fitted well the closed-time distribution.

Other types of channels were seen occasionally but their occurrence was too low to permit analysis. The most frequent of these was recorded in cell-attached patches, had a low conductance (7 pS) and a linear *I-V* relation, and the current reversed at $V_p$ near −60 mV.

## DISCUSSION

### *Origin of K and Cl Channels*

The epithelium of the frog skin consists of four to six layers of principal cells in addition to flask-shaped mitochondria-rich cells (Voûte and Meier, 1978). The underlying dermis contains several types of glands with ducts opening into the apical surface (Voûte, 1963; Farquhar and Palade, 1964). In the collagenase split epithelium most of the glands are destroyed (Voûte and Meier, 1978; Thompson and Mills, 1981) but some isolated gland cells may remain attached to the epithelium. Mitochondria-rich cells comprise ~1–5% of the apical surface area and of the total cell volume of frog and toad skin epithelia (Voûte and Meier, 1978; Larsen, Ussing, and Spring, 1987). Most cells in the preparation used in these studies had a granular appearance, although occasionally a small number of flask-shaped cells were present. Patches were tried only in the larger, granular cells. Given the large proportion of principal cells most patches in this study were necessarily from these, although it is not possible to firmly rule out that other cell types were patched on occasions. Some of the single channel recordings were done in cells in the periphery of large clusters and the results were not different from those obtained in isolated, rounded cells.

In the intact epithelium the principal cells responsible for the active absorption of Na are interconnected by gap junctions (Farquhar and Palade, 1964). Only the outer facing (apical) membrane of the outermost living cell layer (*Stratum granulosum*) contains Na-selective, amiloride-sensitive channels, while Na-K ATPase and K channels are distributed on the basolateral membrane of this cell layer and on the cell membranes of the innermost layers (Farquhar and Palade, 1966; Mills et al., 1977). The polarity is maintained by the tight junctions between cells of the outer *S. granulosum,* which also restricts diffusion between the outer solution and the intercellular spaces (Martínez-Palomo, Erlij, and Bracho, 1971). These structural observations, together with the demonstration of the syncytial behavior of the epithelium (Rick et al., 1978) and the large capacitance of the basolateral membrane of the intact epithelium (Smith, 1971; García-Díaz and Essig, 1985; Schoen and Erlij, 1985) indicates that, functionally, all innermost cell membranes behave as basolateral

membrane. This implies that the majority of isolated cells will exhibit macroscopic properties that correspond to the basolateral membrane of the intact epithelium and there would be a much higher probability of recording single channels of basolateral origin.[2] One can also make the argument that, since the apical membrane of *R. pipiens* skin does not exhibit any significant conductive permeability to ions other than Na (Helman and Fisher, 1977; Nagel, 1977; García-Díaz et al., 1985; Stoddard, Jakobsson, and Helman, 1985; Dörge, Beck, Wienecke, and Rick, 1989) the K and Cl selective channels found in this study are necessarily of basolateral origin.

*K Currents*

Most of the conductance of isolated frog skin cells was due to K and was blocked by Ba and quinidine. In some cases there was a Cl-dependent component of the outward current that was inhibited by DPC, but no Na-dependent current could be demonstrated. Whole-cell currents did not show any clear activation or inactivation kinetics. Because the K currents were active at all potentials it was not possible to correct for leak due to conduction through unspecified background ion channels or the membrane-pipette seal. It is possible to make a crude estimation of the leak if one assumes that most of the current at the most negative voltage (−160 mV) in the presence of 5 mM Ba is due to leak, and that the leak current varies linearly with voltage, reversing at 0 mV with high external K. With these assumptions the leak conductance was estimated to be 1.2 ± 0.8 nS ($n$ = 8); i.e., 24% of the total cell conductance.

With K gluconate in the bath the *I-V* relations were near linear or had a weak inward rectification (Figs. 1–3), less pronounced than that shown by the single K channel currents. When comparing the whole-cell and single channel *I-V* relations one has to consider that the presence of a linear leak will make the observed whole-cell currents less rectifying. In addition, the expected macroscopic current originating from an ensemble of the K channels described here will be less rectifying than the single channel current due to the decrease of open probability with hyperpolarization (see Fig. 8 *C* and Eq. 4). The product of single channel current and open probability ($i \cdot f$) for the four experiments of Fig. 8 varied almost linearly with membrane voltage in the range −20 to −120 mV.

A salient feature of the whole-cell currents was the crossover of outward currents when K was substituted for Na or NMDG in the bath. Such behavior is contrary to that expected from a Goldman-Hodgkin-Katz model, which predicts an asymptotic approach of the currents at high positive voltages when most of the outward current is due to K efflux from the cell. Even assuming that the leak component in the presence of high external K increases to 24% of the total current (which is the maximum leak current estimated under these conditions) crossover of the corrected outward currents persists, but at more positive potentials. The conclusion then is that high external K stimulates K efflux. Such effect is predicted by multi-ion models of permeation (Hille and Schwarz, 1978) where independence of ion fluxes is not obeyed. In striated muscle, raising the external K increases K efflux through the

[2]Although there is a low probability of finding a Na channel of apical origin they would be undetected since most single channel recordings were done with KCl-filled pipettes.

inward rectifier (Adrian, 1962; Horowicz, Gage, and Eisenberg, 1968; Spalding, Senyk, Swift, and Horowicz, 1981), resulting in a crossover of outward currents (Noble and Tsien, 1968; Adrian, 1969). Crossover of the *I-V* relations are also evident for single channel currents measured at varying pipette K concentrations for inward rectifier channels of MDCK cells (Friedrich, Weiss, Paulmichl, and Lang, 1989) and basolateral membrane of rabbit proximal tubule cells (Parent, Cardinal, and Sauvé, 1988). Indeed these inward rectifier channels show many similarities to the K channel described here, as will be discussed later. A multi-ion permeation mechanism is common for K channels (Hille and Schwarz, 1978; Latorre and Miller, 1983) and it has also been proposed for the apical K channel found in the skin of *R. temporaria* (Zeiske and Van Driessche, 1983).

Voltage-dependent blockade by Ba is generally described in terms of a Woodhull (1973) model which predicts a Boltzmann relation between the probability of being unblocked ($I_{Ba}/I$) and membrane voltage (Standen and Stanfield, 1978; Vergara and Latorre, 1983; Moczydlowski, 1986; Giebisch, Hunter, and Kawahara, 1990). The ratio of total currents in the present experiments (Fig. 2 *D*) followed this relation although there were instances in which the inhibition was less than expected at very negative voltages, probably as a consequence of the presence of leak, as noted before. But there was also some inhibition at large positive voltages that failed to fit the equation. This could arise either by the presence of a voltage-independent blockade by Ba of the background or leak conductance, or by the existence of a second blocking site located outside the electrical field of the channel itself. A third possibility is that Ba is able to penetrate the cell membrane and block from the inside. Since internal Ba blocks at concentrations about four orders of magnitude lower than those required for external block (Eaton and Brodwick, 1980; Miller, Latorre, and Reisin, 1987) only a small amount of Ba would need to cross into the cell. The present experiments do not distinguish between these possibilities. In contrast to the present findings, in cells of the early distal tubule of frog kidney Ba has a dual effect on whole-cell currents, inhibiting inward but stimulating outward currents (Hunter, Obertleithner, Henderson, and Giebisch, 1988). The reason for that behavior is not known.

Fitting to the Boltzmann relation gave an average value of $\delta = 0.3$, comparable to values found in other preparations for external Ba blockade (Vergara and Latorre, 1983; Giebisch et al., 1990), although lower than in frog muscle inward rectifier (Standen and Stanfield, 1978). The dissociation constant at 0 mV was higher in the present study (27 mM) than in these other cases (range 0.3–1.8 mM). A simple interpretation of $\delta = 0.3$ is that Ba binds at a site located about one third into the membrane electrical field. However, since there is evidence that the K channel responsible for most of the whole-cell currents operates by a multiion mechanism, the effective valence of blocking ($\delta z$) might be higher than that expected from the physical position of the site, due to coupling of movement of conducting and blocking ions (Hille and Schwarz, 1978; Miller et al., 1987).

At the single channel level the event most frequently observed in cell attached patches was a K channel with an inwardly rectifying *I-V* relation. The single channel conductance, 44 pS at the reversal potential, is in the midrange for K channels. The kinetic behavior of the channel was characterized by bursts of openings separated by

long shut periods. At $V_p = 0$ the kinetics was described by a single open state with a mean open time of 8 ms and at least two closed states. Only a fast closed component (with $\tau_c = 1.6$ ms) could be measured, but it was clear from the current records that at least an additional closed state (with long shut periods) was present. The open probability of the channel was on average 0.62 at $V_p = 0$ and increased with depolarization, but the extent of the voltage dependence was quite variable among experiments. These characteristics are common to K channels found in several epithelial preparations, such as basolateral membranes of turtle colon (Richards and Dawson, 1986), rabbit proximal convoluted (Parent et al., 1988) and straight renal tubules (Gögelein and Greger, 1987), dogfish rectal gland (Greger, Gogelein, and Schlatter, 1987*a*), subconfluent MDCK cells (Friedrich, Paulmichl, Kolb, and Lang, 1988; Friedrich et al., 1989), and apical membranes of thick ascending limb of rat kidney (Bleich, Schlatter, and Greger, 1990; Greger, Bleich, and Schlatter, 1990). All these channels exhibit inward rectification, conductances in the range 50–70 pS with high K on both sides of the patch, and, where analyzed, an open time constant of ~10 ms, at least two closed time constants, the smaller ~1 ms, and a weak increase of the open probability with depolarization. In basolateral membranes of the canine tracheal epithelium (Welsh and McCann, 1985) and apical thick ascending limb of rabbit kidney (Wang, White, Geibel, and Giebisch, 1990) the K channel conductance was only 20–25 pS. The conduction and/or kinetics characteristics differ, however, in some other basolateral K channels: rabbit urinary bladder (Lewis and Hanrahan, 1985) and distal convoluted renal tubule (Taniguchi, Yoshitomi, and Imai, 1989), *Necturus* proximal tubule (Hunter, Kawahara, and Giebisch, 1986; Kawahara, Hunter, and Giebisch, 1987; Sackin and Palmer, 1987), intestine (Sheppard, Giráldez, and Sepúlveda, 1988) and gallbladder (Wehner, Garretson, Dawson, Segal, and Reuss, 1990), and human nasal airway epithelium (Kunzelmann, Pavenstädt, Beck, Unal, Emmrich, Arndt, and Greger, 1989*a*).

Excision of the patch resulted in an immediate inactivation of the K channel. Such inactivation has been observed previously in several channel types, including epithelial K channels from basolateral membrane of turtle colon (Richards and Dawson, 1986) and rabbit proximal convoluted renal tubule (Parent et al., 1988) and points to the presence of some activating factor that is lost after excision. Quantification of the selectivity of the channel would have required changes in the composition of the pipette solutions, but such an approach has not been yet attempted due to the low probability of finding active patches in this preparation. For the same reasons, the study of Ba blockade on the single channel would have required addition of Ba to the pipette solutions, but the variability in channel kinetics among experiments made this approach unfeasible. Quinidine, on the other hand, did not present such problems since at a pH of 7.6, 9% of the drug is in neutral form and is permeable through the cell membrane (Hermann and Gorman, 1984). Both quinidine and its stereoisomer quinine had been shown to inhibit a variety of K channels. At the single channel level different types of blockade (fast, slow, or intermediate) by either of these compounds have been described, depending on the kind of K channel affected. Thus, in inward rectifier, ATP-sensitive and delayed rectifier K channels (Richards and Dawson, 1986; Gögelein, Greger, and Schlatter, 1987; Bokvist, Rorsman, and Smith, 1990*a*, *b*) the blockade is similar to that found in the present experiments,

being slow or intermediate with no reduction of the channel amplitude. On the other hand, in Ca-sensitive K channels (Glavinovic and Trifaró, 1988; Bleich et al., 1990; Bokvist et al., 1990*b*; Mancilla and Rojas, 1990; Segal and Reuss, 1990) or nonselective cation channels (Rae, Dewey, Cooper, and Gates, 1990*a*) the blockade is fast with a reduction in channel amplitude. In those cases where the kinetics was analyzed (Glavinovic and Trifaró, 1988; Bokvist et al., 1990*a*; Mancilla and Rojas, 1990) the results are consistent with a sequential model where the drug binds to the channel in the open state, as found in the present experiments. Also in agreement with the results obtained here for whole-cell K currents (Fig. 3), the blockade was found to be either voltage independent (Bokvist et al., 1990*a*; Segal and Reuss, 1990) or with a weak voltage dependency (Glavinovic and Trifaró, 1988; Rae et al., 1990*a*).

It is very likely that this K channel is the major component of the whole-cell currents recorded in high external K. In favor of this possibility are the similarities between the *I-V* relations of the whole-cell and single channel currents, the strong inhibition by quinidine of both currents, and the observation that this channel was by far the most frequent of the microscopic events recorded. With this hypothesis it is possible to estimate the number of channels in a cell from the relation:

$$g = N \gamma f \tag{3}$$

where $g$ and $\gamma$ are the whole-cell and single channel conductances, $N$ is the number of channels per cell, and $f$ the fractional open time of a single channel (open probability). Using the average values at 0 mV of $g$ = 3.8 nS (corrected for leak conductance), $\gamma$ = 44 pS, and $f$ of 0.8 (extrapolating from Fig. 8 *C* to reversal potential), the calculated $N$ is 108 channels/cell. For a cell of 25 μm diameter this amounts to about one channel per 20 $\mu m^2$, consistent with the low number of active patches found in this preparation. It is difficult to compare these values with the basolateral conductance of the intact epithelium due to the complex morphology involving multiple cell layers and infoldings of the cell membranes. There are, however, certain resemblances between the basolateral conductance of the intact epithelium and the present results. Basolateral *I-V* relations in the intact epithelium, measured with transepithelial voltage pulses of 400–600 ms in Na medium, are linear or have a slight outward rectification at depolarized or positive voltages (Schoen and Erlij, 1985; Nagel et al., 1988). Such behavior is comparable to that of the whole-cell currents in Na medium reported here in the voltage range between reversal and 20 mV. Another similarity is the inhibition of basolateral conductance of the frog skin epithelium by Ba (Nagel, 1979) and quinidine (Abramcheck, Gupta, Sabatini, and Helman, 1982; Van Driessche and Hillyard, 1985; García-Díaz, J. F., unpublished data).

### *Cl Currents*

In the presence of high external Cl an outward current component appeared that was inhibited by addition of the anion channel blocker DPC. These observations do not necessarily imply the presence of a Cl current since there are reports showing that K channels are stimulated by external Cl (Rae, Dewey, Cooper, and Gates, 1990*b*) and inhibited by DPC (Chang and Dawson, 1988; Richards and Dawson, 1989). However, the Cl-dependent component of the current, obtained as the difference in currents in

the absence and presence of DPC, exhibited a marked outward rectification, similar to that of the single Cl channel (compare Figs. 4 *D* and 12). Also, the reversal potentials (− 41 ± 4 mV) agreed with the calculated Cl equilibrium potential (−39 mV). These observations suggest the presence of a Cl conductive pathway in epithelial cells of frog skin. For reasons already discussed it is most likely of basolateral origin. The Cl current was observed in ~70% of the cells. It is not known what mechanisms activate the current but, from the similarities to other epithelial systems, cell swelling induced by equilibration of the cell contents with the pipette solution could be a factor. As will be discussed later, the Cl channel described here shows many similarities to the outwardly rectifying anion channel found in airway epithelia, where whole-cell currents sustained by the anion channel are greatly stimulated by decreases in bath tonicity (McCann, Li, and Welsh, 1989; McCann and Welsh, 1990). Similarly, an outwardly rectifying Cl current activated by cell swelling has been described in $T_{84}$ colonic cells (Worrell, Butt, Cliff, and Frizzell, 1989). Although the basolateral membrane of frog skin is normally tight to Cl (Giráldez and Ferreira, 1984; Nagel, 1985), it has been proposed that cell swelling and/or depolarization activates a Cl conductance in this membrane as part of a mechanism of regulatory volume decrease (Ussing, 1982, 1986). Activation of basolateral Cl channels has been deemed essential for volume regulation in a mathematical model of tight epithelia (Strieter, Stephenson, Palmer, and Weinstein, 1990). It is tentatively concluded, then, that the main role of the basolateral Cl conductance described here is in the regulation of cellular volume. This conductance is *not* involved in the transepithelial absorption of Cl that takes place in the frog skin in vivo or in vitro under open circuit conditions. Movement of Cl does not occur through the Na-transporting principal cells of the epithelium (García-Díaz et al., 1985; Dörge et al., 1989) but seems to be localized either in the mitochondria-rich cells (Voûte and Meier, 1978; Foskett and Ussing, 1986; Larsen et al., 1987) or in the tight junctions between *Stratum granulosum* cells (Nagel, 1989; Nagel and Dörge, 1990).

The Cl channel described here shows many striking similarities to the outwardly rectifying anion channel found in many other epithelia (Gögelein, 1988; Tabcharani, Jensen, Riordan, and Hanrahan, 1989). These similar characteristics are an outwardly rectifying *I-V* relation, conductance of near 50 pS at 0 mV with symmetrical 112 mM Cl solutions, at least two open and two closed states and an open probability that increases with depolarization. In most cases this anion channel has been found at the apical membranes of secretory epithelia: trachea (Frizzell, Rechkemmer, and Shoemaker, 1986; Welsh, 1986*a*, *b*; Welsh and Liedtke, 1986), dogfish rectal gland (Greger, Schlatter, and Gögelein, 1987*b*), $T_{84}$ colonic cell line (Halm, Rechkemmer, Schoumacher, and Frizzell, 1988; Tabcharani et al., 1989), cultured nasal airway (Kunzelmann, Pavestädt, and Greger, 1989*b*), pancreatic duct cell lines (Tabcharani et al., 1989; Schoumacher, Ram, Iannuzzi, Bradbury, Wallace, Hon, Kelly, Schmid, Gelder, Rado, and Frizzell, 1990), and sweat glands (Krouse, Hagiwara, Chen, Lewinston, and Wine, 1989; Tabcharani et al., 1989). It has also been observed at the basolateral membrane of the rat thick ascending limb of Henle's loop (Greger et al., 1990). Defective regulation of this channel in airway epithelia plays a major role in the impaired secretion found in cystic fibrosis (Frizzell et al., 1986; McCann and Welsh, 1990). Another similarity with the anion channel of airway epithelia is the

activation by excision and strong depolarization (Frizzell et al., 1986; Welsh, 1986*a*). The mechanism for this activation is not known (McCann and Welsh, 1990). The voltage dependence of the open probability for the channel described here is, however, much stronger than for the other preparations mentioned, with perhaps the exception of the channel in sweat glands described by Krouse et al. (1989). These authors found that the voltage dependence resulted from a shift from the mainly closed mode at hyperpolarized potentials to the mainly open mode at depolarized potentials. Such a description also seems to apply to the behavior of the Cl channel described here (see Fig. 11). The conduction and/or kinetic properties differ from basolateral Cl channels of rabbit urinary bladder (Hanrahan, Alles, and Lewis, 1985; Lewis and Hanrahan, 1985) and cortical collecting ducts (Sansom, La, and Carosi, 1990).

Because of the infrequent observation of this channel the effect of DPC was not tested. It is very likely, however, that it is responsible for the Cl component of the whole-cell currents. This is supported by the similar outward rectification of both the single channel current and the Cl- and DPC-sensitive component of the whole-cell currents. But the actual identification of the single channel responsible for this component of the whole-cell current as well as its possible role in cell volume regulation, requires further investigation.

I am indebted to Dr. E. Nasi for his advice on many aspects of this work and for numerous discussions. I am also thankful to Dr. E. Nasi and Dr. G. Jones for reviewing the manuscript.

This work was supported by a grant from the National Institutes of Health (DK-39214).

*Original version received 19 October 1990 and accepted version received 14 February 1991.*

## REFERENCES

Abramcheck, F., S. Gupta, S. Sabatini, and S. Helman. 1982. Mechanism of action of quinine on Na transport in frog skin. *Federation Proceedings.* 41:1349. (Abstr.)

Adrian, R. H. 1962. Movement of inorganic ions across the membrane of striated muscle. *Circulation.* 26:1214–1223.

Adrian, R. H. 1969. Rectification in muscle membrane. *Progress in Biophysics and Molecular Biology.* 19:339–369.

Bleich, M., E. Schlatter, and R. Greger. 1990. The luminal $K^+$ channel of the thick ascending limb of Henle's loop. *Pflügers Archiv.* 415:449–460.

Bokvist, K., P. Rorsman, and P. A. Smith. 1990*a*. Effects of external tetraethylammonium ions and quinine on delayed rectifying $K^+$ channels in mouse pancreatic B-cells. *Journal of Physiology.* 423:311–325.

Bokvist, K., P. Rorsman, and P. A. Smith. 1990*b*. Block of ATP-regulated and $Ca^{2+}$-activated $K^+$ channels in mouse pancreatic B-cells by external tetraethylammonium and quinine. *Journal of Physiology.* 423:327–342.

Chang, D., and D. C. Dawson. 1988. Digitonin-permeabilized colonic cell layers. Demonstration of calcium-activated basolateral K and Cl conductances. *Journal of General Physiology.* 92:281–306.

Colquhoun, D., and A. C. Hawkes. 1983. The principles of the stochastic interpretation of ion-channel mechanisms. *In* Single Channel Recording. B. Sakmann and E. Neher, editors. Plenum Publishing Corp., New York. 135–175.

Dawson, D. C., and N. W. Richards. 1990. Basolateral K conductance: role in regulation of NaCl absorption and secretion. *American Journal of Physiology.* 259:C181–C195.

Di Stefano, A., M. Wittner, E. Schlatter, H. J. Lang, H. Englert, and R. Greger. 1985. Diphenylamine-2-carboxylate, a blocker of the Cl-conductive pathway in Cl-transporting epithelia. *Pflügers Archiv.* 405(Suppl. 1):S95–S100.

Dörge, A., F. X. Beck, P. Wienecke, and R. Rick. 1989. Cl transport across the basolateral membrane of principal cells in frog skin. *Mineral Electrolyte and Metabolism.* 15:155–162.

Eaton, D. C., and M. S. Brodwick. 1980. Effect of barium on the potassium conductance of squid axons. *Journal of General Physiology.* 75:727–750.

Farquhar, M. G., and G. E. Palade. 1964. Cell junctions in amphibian skin. *Journal of Cell Biology.* 26:263–291.

Farquhar, M. G., and G. E. Palade. 1966. Adenosine triphosphatase localization in amphibian epidermis. *Journal of Cell Biology.* 30:359–379.

Fisher, R. S., D. Erlij, and S. I. Helman. 1980. Intracellular voltage of isolated epithelia of frog skin. Apical and basolateral cell punctures. *Journal of General Physiology.* 76:447–453.

Foskett, J. K., and H. H. Ussing. 1986. Localization of chloride conductance to mitochondria-rich cells in frog skin epithelium. *Journal of Membrane Biology.* 91:251–258.

Friedrich, F., M. Paulmichl, H. A. Kolb, and F. Lang. 1988. Inward rectifier K channels in renal epithelioid cells (MDCK) activated by serotonin. *Journal of Membrane Biology.* 106:149–155.

Friedrich, F., H. Weiss, M. Paulmichl, and F. Lang. 1989. Activation of potassium channels in renal epitheloid cells (MDCK) by extracellular ATP. *American Journal of Physiology.* 256:C1016–C1021.

Frizzell, R. A., G. Rechkemmer, and R. L. Shoemaker. 1986. Altered regulation of airway epithelial cell chloride channels in cystic fibrosis. *Science.* 233:558–560.

García-Díaz, J. F. 1990. Single K channel at the basolateral membrane of frog skin epithelium. *Biophysical Journal.* 57:84a. (Abstr.)

García-Díaz, J. F., L. M. Baxendale, G. Klemperer, and A. Essig. 1985. Cell K activity in frog skin in the presence and absence of cell current. *Journal of Membrane Biology.* 85:143–158.

García-Díaz, J. F., and A. Essig. 1985. Capacitative transients in voltage-clamped epithelia. *Biophysical Journal.* 48:519–523.

Giebisch, G., M. Hunter, and K. Kawahara. 1990. Apical potassium channels in Amphiuma diluting segment: effect of barium. *Journal of Physiology.* 420:313–323.

Giráldez, F., and K. T. G. Ferreira. 1984. Intracellular chloride activity and membrane potential in stripped frog skin (*Rana temporaria*). *Biochimica et Biophysica Acta.* 769:625–628.

Glavinovic, M. I., and J. M. Trifaró. 1988. Quinine blockade of currents through $Ca^{2+}$-activated $K^+$ channels in bovine chromaffin cells. *Journal of Physiology.* 399:139–152.

Gögelein, H. 1988. Chloride channels in epithelia. *Biochimica et Biophysica Acta.* 947:521–547.

Gögelein, H., and R. Greger. 1987. Properties of single $K^+$ channels in the basolateral membrane of rabbit proximal straight tubules. *Pflügers Archiv.* 410:288–295.

Gögelein, H., R. Greger, and E. Schlatter. 1987. Potassium channels in the basolateral membrane of the rectal gland of Squalus acanthias. Regulation and inhibitors. *Pflügers Archiv.* 409:107–113.

Greger, R., M. Bleich, and E. Schlatter. 1990. Ion channels in the thick ascending limb of Henle's loop. *Renal Physiology and Biochemistry.* 13:37–50.

Greger, R., H. Gögelein, and E. Schlatter. 1987*a*. Potassium channels in the basolateral membrane of the rectal gland of the dogfish (*Squalus acanthias*). *Pflügers Archiv.* 409:100–106.

Greger, R., E. Schlatter, and H. Gögelein. 1987*b*. Chloride channels in the luminal membrane of the rectal gland of the dogfish (*Squalus acanthias*). *Pflügers Archiv.* 409:114–121.

Halm, D. R., G. R. Rechkemmer, R. A. Schoumacher, and R. A. Frizzell. 1988. Apical membrane chloride channels in a colonic cell line activated by secretory agonists. *American Journal of Physiology.* 254:C505–C511.

Hamill, O. P., A. Marty, E. Neher, B. Sackman, and F. J. Sigworth. 1981. Improved patch-clamp techniques for high-resolution current recording from cells and cell-free membrane patches. *Pflügers Archiv.* 91:85–100.

Hanrahan, J. W., W. P. Alles, and S. A. Lewis. 1985. Single anion-selective channels in basolateral membrane of a mammalian tight epithelium. *Proceedings of the National Academy of Sciences.* 82:7791–7795.

Helman, S. I., and R. S. Fisher. 1977. Microelectrode studies of the active Na transport pathway of frog skin. *Journal of General Physiology.* 69:571–604.

Hermann, A., and A. L. F. Gorman. 1984. Action of quinidine on ionic currents of molluscan pacemaker neurons. *Journal of General Physiology.* 83:919–940.

Hille, B., and W. Schwarz. 1978. Potassium channels as multi-ion single-file pores. *Journal of General Physiology.* 72:409–442.

Horn, R., and A. Marty. 1988. Muscarinic activation of ionic currents measured by a new whole-cell recording method. *Journal of General Physiology.* 92:145–159.

Horowicz, P., P. W. Gage, and R. S. Eisenberg. 1968. The role of the electrochemical gradient in determining potassium fluxes in frog striated muscle. *Journal of General Physiology.* 51:193s–203s.

Hunter, M., K. Kawahara, and G. Giebisch. 1986. Potassium channels along the nephron. *Federation Proceedings.* 45:2723–2726.

Hunter, M., H. Oberleithner, R. M. Henderson, and G. Giebisch. 1988. Whole-cell potassium currents in single early distal tubule cells. *American Journal of Physiology.* 255:F699–F703.

Kawahara, K., M. Hunter, and G. Giebisch. 1987. Potassium channels in *Necturus* proximal tubule. *American Journal of Physiology.* 253:F488–F494.

Koefoed-Johnsen, V., and H. H. Ussing. 1958. The nature of the frog skin potential. *Acta Physiologica Scandinavica.* 42:298–308.

Krouse, M. E., G. Hagiwara, J. Chen, N. J. Lewinston, and J. J. Wine. 1989. Ion channels in normal human and cystic fibrosis sweat gland cells. *American Journal of Physiology.* 257:C129–C140.

Kunzelmann, K., H. Pavenstädt, C. Beck, O. Unal, P. Emmrich, H. J. Arndt, and R. Greger. 1989*a*. Characterization of potassium channels in respiratory cells. I. General properties. *Pflügers Archiv.* 414:291–296.

Kunzelmann, K., H. Pavenstädt, and R. Greger. 1989*b*. Properties and regulation of chloride channels in cystic fibrosis and normal airway cells. *Pflügers Archiv.* 415:172–182.

Larsen, E. H., H. H. Ussing, and K. R. Spring. 1987. Ion transport by mitochondria-rich cells in toad skin. *Journal of Membrane Biology.* 99:25–40.

Latorre, R., and C. Miller. 1983. Conduction and selectivity in potassium channels. *Journal of Membrane Biology.* 71:11–30.

Lewis, S. A., and J. W. Hanrahan. 1985. Apical and basolateral membrane ionic channels in rabbit urinary bladder epithelium. *Pflügers Archiv.* 405(Suppl. 1):S83–S88.

Mancilla, E., and E. Rojas. 1990. Quinine blocks the high conductance, calcium-activated potassium channel in rat pancreatic β-cells. *FEBS (Federation of European Biochemical Societies) Letters.* 260:105–108.

Martinez-Palomo, A., D. Erlij, and H. Bracho. 1971. Localization of permeability barriers in the frog skin epithelium. *Journal of Cell Biology.* 50:277–287.

McCann, J. D., M. Li, and M. J. Welsh. 1989. Identification and regulation of whole-cell chloride currents in airway epithelium. *Journal of General Physiology.* 94:1015–1036.

McCann, J. D., and M. J. Welsh. 1990. Regulation of $Cl^-$ and $K^+$ channels in airway epithelium. *Annual Review of Physiology.* 52:115–135.

Miller, C., R. Latorre, and I. Reisin. 1987. Coupling of voltage-dependent gating and $Ba^{++}$ block in the high-conductance $Ca^{++}$-activated $K^+$ channel. *Journal of General Physiology.* 90:427–449.

Mills, J. W., S. A. Ernst, and D. R. DiBona. 1977. Localization of $Na^+$-pump sites in frog skin. *Journal of Cell Biology.* 73:88–110.

Moczydlowski, E. 1986. Single-channel enzymology. *In* Ion Channel Reconstitution. C. Miller, editor. Plenum Publishing Corp., New York. 75–113.

Nagel, W. 1977. The dependence of the electrical potentials across the membranes of the frog skin upon the concentration of sodium in the mucosal solution. *Journal of Physiology.* 269:777–796.

Nagel, W. 1979. Inhibition of potassium conductance by barium in frog skin epithelium. *Biochimica et Biophysica Acta.* 552:346–357.

Nagel, W. 1985. Basolateral membrane ionic conductance in frog skin. *Pflügers Archiv.* 405 (Suppl. 1): S39–S43.

Nagel, W. 1989. Chloride conductance of frog skin: localization to the tight junctions? *Mineral and Electrolyte Metabolism.* 15:163–170.

Nagel, W., and A. Dörge. 1990. Analysis of anion conductance in frog skin. *Pflügers Archiv.* 416:53–61.

Nagel, W., J. F. García-Díaz, and W. McD. Armstrong. 1981. Intracellular ionic activities in frog skin. *Journal of Membrane Biology.* 61:127–134.

Nagel, W., J. F. García-Díaz, and A. Essig. 1988. Voltage dependence of cellular current and conductances in frog skin. *Journal of Membrane Biology.* 106:13–28.

Noble, D., and R. W. Tsien. 1968. The kinetics and rectifier properties of the slow potassium current in cardiac Purkinje fibres. *Journal of Physiology.* 195:185–214.

Parent, L., J. Cardinal, and R. Sauvé. 1988. Single-channel analysis of a K channel at basolateral membrane of rabbit proximal convoluted tubule. *American Journal of Physiology.* 254:F105–F113.

Rae, J. L., J. Dewey, K. Cooper, and P. Gates. 1990*a*. A non-selective cation channel in rabbit corneal endothelium activated by internal calcium and inhibited by internal ATP. *Experimental Eye Research.* 50:373–384.

Rae, J. L., J. Dewey, K. Cooper, and P. Gates. 1990*b*. Potassium channel in rabbit corneal endothelium activated by external anions. *Journal of Membrane Biology.* 114:29–36.

Richards, N. W., and D. C. Dawson. 1986. Single potassium channels blocked by lidocaine and quinidine in isolated turtle colon epithelial cells. *American Journal of Physiology.* 251:C85–C89.

Richards, N. W., and D. C. Dawson. 1989. *N*-phenylanthranilic acid blocks specific classes of K-conducting channels in colonic epithelial cells. *FASEB (Federation of American Societies for Experimental Biology) Journal.* 3:A1149. (Abstr.)

Rick, R., A. Dörge, E. Arnim, and K. Thurau. 1978. Electron microprobe analysis of frog skin epithelium: evidence for a syncytial sodium transport compartment. *Journal of Membrane Biology.* 39:313–331.

Sackin, H., and L. Palmer. 1987. Basolateral potassium channels in renal proximal tubule. *American Journal of Physiology.* 253:F476–F487.

Sansom, S. C., B.-Q. La, and S. L. Carosi. 1990. Double-barrelled chloride channels of collecting duct basolateral membrane. *American Journal of Physiology.* 259:F46–F52.

Schoen, H. F., and D. Erlij. 1985. Current-voltage relations of the apical and basolateral membranes of the frog skin. *Journal of General Physiology.* 86:257–287.

Schoumacher, R. A., J. Ram, M. C. Iannuzzi, N. A. Bradbury, R. W. Wallace, C. T. Hon, D. R. Kelly, S. M. Schmid, F. B. Gelder, T. A. Rado, and R. A. Frizzell. 1990. A cystic fibrosis pancreatic adenocarcinoma cell line. *Proceedings of the National Academy of Sciences.* 87:4012–4016.

Segal, Y., and L. Reuss. 1990. $Ba^{2+}$, $TEA^+$, and quinine effects on apical membrane $K^+$ conductance and maxi $K^+$ channels in gallbladder epithelium. *American Journal of Physiology.* 259:C56–C68.

Sheppard, D. N., F. Firáldez, and F. V. Sepúlveda. 1988. Kinetics of voltage- and Ca activation and Ba blockade of a large-conductance K channel from Necturus enterocytes. *Journal of Membrane Biology.* 105:65–75.

Smith, P. G. 1971. The low-frequency electrical impedance of the isolated frog skin. *Acta Physiologica Scandinavica.* 81:355–366.

Spalding, B. C., O. Senyk, J. G. Swift, and P. Horowicz. 1981. Unidirectional flux ratio for potassium ions in depolarized frog skeletal muscle. *American Journal of Physiology.* 241:C68–C75.

Standen, N. B., and P. R. Stanfield. 1978. A potential- and time-dependent blockade of inward rectification in frog skeletal muscle fibres by barium and strontium ions. *Journal of Physiology.* 280:169–191.

Stoddard, J. S., E. Jakobsson, and S. I. Helman. 1985. Basolateral membrane chloride transport in isolated epithelia of frog skin. *American Journal of Physiology.* 249:C318–C329.

Strieter, J., J. L. Stephenson, L. G. Palmer, and A. M. Weinstein. 1990. Volume-activated chloride permeability can mediate cell volume regulation in a mathematical model of a tight epithelium. *Journal of General Physiology.* 96:319–344.

Tabcharani, J. A., T. J. Jensen, J. R. Riordan, and J. W. Hanrahan. 1989. Bicarbonate permeability of the outwardly rectifying anion channel. *Journal of Membrane Biology.* 112:109–122.

Taniguchi, J., K. Yoshitomi, and M. Imai. 1989. $K^+$ channel currents in basolateral membrane of distal convoluted tubule of rabbit kidney. *American Journal of Physiology.* 256:F246–F254.

Thompson, I. G., and J. W. Mills. 1981. Isoproterenol-induced current changes in glands of frog skin. *American Journal of Physiology.* 241:C250–C257.

Ussing, H. H. 1982. Volume regulation of frog skin epithelium. *Acta Physiologica Scandinavica.* 114:363–369.

Ussing, H. H. 1986. Epithelial cell volume regulation illustrated by experiments in frog skin. *Renal Physiology.* 9:38–46.

Ussing, H. H., and K. Zerahn. 1951. Active transport of sodium as the source of electric current in the short-circuited isolated frog skin. *Acta Physiologica Scandinavica.* 23:110–127.

Van Driessche, W., and S. D. Hillyard. 1985. Quinidine blockage of K channels in the basolateral membrane of larval bullfrog skin. *Pflügers Archiv.* 405 (Suppl. 1):S77–S82.

Vergara, C., and R. Latorre. 1983. Kinetics of $Ca^{2+}$-activated $K^+$ channels from rabbit muscle incorporated into planar bilayers. Evidence for a $Ca^{2+}$ and $Ba^{2+}$ blockade. *Journal of General Physiology.* 82:543–568.

Voûte, C. L. 1963. An electron microscopic study of the skin of the frog (*Rana pipiens*). *Journal of Ultrastructural Research.* 9:497–510.

Voûte, C. L., and W. Meier. 1978. The mitochondria-rich cell of frog skin as hormone-sensitive "shunt-path." *Journal of Membrane Biology.* 40(Special Issue):151–165.

Wang, W., S. White, J. Geibel, and G. Giebisch. 1990. A potassium channel in the apical membrane of rabbit thick ascending limb of Henle's loop. *American Journal of Physiology.* 258:F244–F253.

Wehner, F., L. Garretson, K. Dawson, Y. Segal, and L. Reuss. 1990. A nonenzymatic preparation of epithelial basolateral membrane for patch-clamp. *American Journal of Physiology.* 258:C1159–C1164.

Welsh, M. J. 1986*a*. An apical-membrane chloride channel in human tracheal epithelium. *Science.* 232:1648–1650.

Welsh, M. J. 1986*b*. Single apical membrane anion channels in primary cultures of canine tracheal epithelium. *Pflügers Archiv.* 407:S116–S122.

Welsh, M. J., and C. M. Liedtke. 1986. Chloride and potassium channels in cystic fibrosis airway epithelia. *Nature.* 322:467–470.

Welsh, M. J., and J. D. McCann. 1985. Intracellular calcium regulates basolateral potasium channels in a chloride-secreting epithelium. *Proceedings of the National Academy of Sciences.* 82:8823–8826.

Wolf, K., and M. C. Quimby. 1964. Amphibian cell culture: permanent cell line from the bullfrog (*Rana catesbiana*). *Science.* 144:1578–1580.

Woodhull, A. 1973. Ionic blockade of sodium channels in nerve. *Journal of General Physiology.* 61:687–708.

Worrell, R. T., A. G. Butt, W. H. Cliff, and R. A. Frizzell. 1989. A volume-sensitive chloride conductance in human colonic cell line T84. *American Journal of Physiology.* 256:C1111–C1119.

Zeiske, W., and W. Van Driessche. 1983. The interaction of "$K^+$-like" cations with the apical $K^+$ channel in frog skin. *Journal of Membrane Biology.* 76:57–72.